Content in fatty acids and carotenoids in phytoplankton blooms during the seasonal sea ice retreat in Hudson Bay complex, Canada

Rémi Amiraux, Johann Lavaud, Kasey Cameron-Bergeron, Lisa Matthes, Ilka Peeken, Christopher Mundy, David Babb, Jean-Eric Tremblay

ELEMENTA
Science of the Anthropocene

Amiraux, R, et al. 2022. Content in fatty acids and carotenoids in phytoplankton blooms during the seasonal sea ice retreat in Hudson Bay complex, Canada. *Elem Sci Anth*, 10: 1. DOI: https://doi.org/10.1525/elementa.2021.00106

RESEARCH ARTICLE

Content in fatty acids and carotenoids in phytoplankton blooms during the seasonal sea ice retreat in Hudson Bay complex, Canada

Rémi Amiraux[1,*], Johann Lavaud[1,2], Kasey Cameron-Bergeron[1], Lisa C. Matthes[1], Ilka Peeken[3], Christopher J. Mundy[4], David G. Babb[4], and Jean-Eric Tremblay[1]

The Hudson Bay complex (HBC) is home to numerous indigenous communities that traditionally have relied heavily on its marine resources. The nutritional quality and stocks of the entire HBC food web depend in large part on the phytoplankton production of bioactive molecules (long chain polyunsaturated fatty acids and carotenoids) and their transfer through trophic levels. The purpose of this study was thus to determine which molecules were produced during spring phytoplankton blooms, as well as the environmental factors driving this production. We investigated 21 stations in 5 sub-regions of the HBC. At the time of sampling, the sub-regions studied had different environmental settings (e.g., ice cover, nutrients, seawater salinity and temperature) conditioning their bloom stages. Pre- and post-bloom stages were associated with relatively low concentrations of bioactive molecules (either fatty acids or carotenoids). In contrast, the highest concentrations of bioactive molecules (dominated by eicosapentaenoic acid and fucoxanthin) were associated with the diatom bloom that typically occurs at the ice edge when silicates remain available. Interestingly, the large riverine inputs in eastern Hudson Bay led to a change in protist composition (larger contribution of Dinophyceae), resulting in lower while more diverse content of bioactive molecules, whether fatty acids (e.g., αα-linolenic acid) or carotenoids (e.g., peridinin). As greater stratification of the HBC is expected in the future, we suggest that a mixotrophic/heterotrophic flagellate-based food web would become more prevalent, resulting in a smaller supply of bioactive molecules for the food web.

Keywords: Hudson Bay complex, Spring phytoplankton bloom, Long chain polyunsaturated fatty acids, Docosahexaenoic acid, Eicosapentaenoic acid, Carotenoid, Fucoxanthin, Peridinin

1. Introduction

Climate-driven alterations of the marine environment are fastest and deepest at the periphery of the Arctic Ocean (Intergovernmental Panel on Climate Change, 2014). These changes are particularly true of the Hudson Bay complex (HBC; including Hudson Bay, James Bay, Hudson Strait and Foxe Basin), a sub-Arctic Canadian inland sea that covers 1.3 million km^2. This ecosystem has been identified as one of the most vulnerable regions to climate change due to its sensitivity to the simultaneous and concomitant effects of warming, acidification, reductions in the extent, thickness and seasonal persistence of sea ice, changes in upper ocean dynamics and increased freshwater loading from precipitation, rivers and melting sea ice (Gagnon and Gough, 2005; Tivy et al., 2011; Derksen et al., 2019; Tremblay et al., 2019). Such disruptions of the HBC ecosystem will have many consequences on the ecosystem services it provides, including provision of food and the maintenance of the biodiversity of habitats and species that sustain this production (Hoover et al., 2013). Indeed, at the base of the food web, the production of organic matter by primary producers (e.g., ice algae, phytoplankton, benthic algae) is driven by the availability of light and nutrients and presumably modulated by other factors such as temperature, salinity, pH and the availability of free carbon dioxide (CO_2; Campbell et al., 2016). Changes in these drivers, particularly due to climate change, are expected to affect the biodiversity of the primary producers (Witman et al., 2008; Wassmann et al., 2011; Vallina et al., 2014), which will influence the quantity and quality of organic matter available for the maintenance

[1] Takuvik International Research Laboratory, Québec Océan, Laval University (Canada) - CNRS, Département de biologie and Québec-Océan, Université Laval, Québec, QC, Canada

[2] UMR6539 LEMAR-Laboratory of Environmental Marine Sciences, CNRS/Univ Brest/Ifremer/IRD, Institut Universitaire Européen de la Mer, Plouzané, France

[3] Alfred Wegener Institute, Helmholtz Centre for Polar and Marine Research, Bremerhaven, Germany

[4] Centre for Earth Observation Science, University of Manitoba, Winnipeg, MB, Canada

* Corresponding author:
Email: remi.amiraux@takuvik.ulaval.ca

of the marine food web (Chassot et al., 2010; Leu et al., 2011; Campanyà-Llovet et al., 2017; Jin et al., 2020).

Phytoplankton provides a very diverse source of bioactive molecules defining the quality of organic matter available for consumers. Among these molecules, fatty acids and pigments play physiological roles that allow cells to cope with changes in environmental constraints; e.g. lipid composition of cell membranes can vary according to environmental factors, and the diversity of light-harvesting pigments allows efficient photosynthesis at different depths in the water column (Brunet et al., 2011; Marmillot et al., 2020). Some of these molecules, such as long-chain polyunsaturated fatty acids (LC-PUFA) and carotenoid pigments, are produced in substantial amounts by primary producers and are essential components for organisms across the entire food web (Hendriks et al., 2003). Thus, marine animals can either directly accumulate LC-PUFA and carotenoids from food or partly modify them through metabolic mechanisms (Hendriks et al., 2003; Galasso et al., 2017).

Long chain polyunsaturated fatty acids are fatty acids of $\geq$20 carbons in length and at least two conjugated double bonds in the *cis* position. LC-PUFA are divided into two main groups, omega-3 (ω-3) and omega-6 (ω-6), which are distinguished by the first double bond position counted from the methyl end at carbon 3 and 6, respectively (Schmidt and Dyerberg, 1994; Ruiz-López et al., 2012). These lipids are essential for the growth and reproduction of most marine animals, which depend on the initial synthesis of LC-PUFA primarily by marine photosynthetic organisms (Nichols, 2003; Søreide et al., 2010; Leu et al., 2011). Phytoplankton taxa differ in their LC-PUFA production (Volkman et al., 1989; Napolitano et al., 1990; Leonardos and Lucas, 2000), allowing for taxonomic protist identification from fatty acid profiles. For instance, C20:5 eicosapentaenoic acid (EPA) is mostly produced by diatoms, while C22:6 docosahexaenoic acid (DHA) is associated with dinoflagellates (Søreide et al., 2008; Poulin et al., 2011; Kelly and Scheibling, 2012). In terms of human health benefits, EPA, DHA and C18:3 αα-linolenic acid (ALA) are the most important ω-3 family LC-PUFAs, whereas in the ω-6 family, C18:2 linoleic acid (LA) and C20:3 ɤ-linoleic acid (GLA) are important (Fan and Chapkin, 1998; Erdinest et al., 2012; Shahidi and Ambigaipalan, 2018). Among these health benefits, LC-PUFA is associated with anti-inflammatory processes (Smith et al., 2011), proper fetal development and healthy aging (Dunstan et al., 2007), and the prevention of many diseases (Robertson et al., 2013; Calder, 2014; Katiyar and Arora, 2020).

Carotenoids are a family of pigmented compounds that are synthesized by photosynthetic microorganisms and plants, where they play a vital function in absorbing light energy for photosynthesis, protecting the photosynthetic apparatus by dissipating the excess light energy, scavenging free radicals and stabilizing cell membranes (Solovchenko and Merzlyak, 2008; Egeland, 2016; Huang et al., 2017). Because of their rapid growth rate and unique carotenoid profiles, phytoplankton taxa are an excellent source of particular carotenoids (Egeland, 2016; Huang et al., 2017) that are absent or at trace levels in higher organisms (bacteria also produce carotenoids against photooxidative stress and for membrane fluidity; Shivaji and Prakash, 2010; Coelho et al., 2022). The uniqueness of the carotenoid profiles of phytoplankton means that carotenoids allow chemotaxonomic identification. For example, diatoms are rich in fucoxanthin while peridinin is the major carotenoid in dinoflagellates (Yoon et al., 2002; Xia et al., 2013; Egeland, 2016; Huang et al., 2017). Also, specific de-epoxidized forms with strong protective functions can be synthesized in response to harsh growing conditions such as high light or low nutrient availability (Alou-Font et al., 2016; Galindo et al., 2017; Lacour et al., 2020). For instance, in Arctic diatoms, the xanthophyll carotenoid diadinoxanthin (DD) is converted to diatoxanthin (DT) in order to prevent and/or reduce the oxidative stress generated by excess light exposure (Kauko et al., 2019; Lacour et al., 2020; Croteau et al., 2021). Because of their health-benefiting properties for human beings, carotenoids have been a major focus of research in recent decades (Yeum et al., 2009; Peng et al., 2011). Indeed carotenoids (i) are important dietary sources of vitamin A (Paiva and Russell, 1999; Galasso et al., 2019), (ii) present antioxidative properties (Galasso et al., 2017; Sansone and Brunet, 2020) and (iii) are thought to prevent human diseases including cardiovascular diseases, cancer and other chronic diseases (Astorg et al., 1997; Paiva and Russell, 1999; Galasso et al., 2019).

Interestingly, the carotenoids and LC-PUFAs produced by phytoplankton would act synergistically, providing an enhanced bioactivity on inflammatory response, and thus on cardiovascular disease risk prevention (Rao and Rao, 2007; Micallef and Garg, 2009; D'Orazio et al., 2012). Hence, any modification in the phytoplankton productivity of carotenoid and LC-PUFAs could be expected to impact the bioavailability of these health-benefiting molecules for the marine food web, directly affecting humans whose nutrition relies upon these marine resources (Leu et al., 2010; Leu et al., 2016). The HBC is home to many indigenous communities (Inuit and Cree) on or near shore that traditionally have relied heavily on its marine resources (Kuzyk and Candlish, 2019). However, to the best of our knowledge, no studies have previously determined the phytoplankton production of the bioactive molecules (LC-PUFA and carotenoids) that define the nutritional quality of the entire HBC marine food web. Our objectives were to determine which molecules were produced during the different phytoplankton bloom stages over the HBC, as well as the protist communities and environmental factors driving their production.

2. Materials and methods

2.1. Study area

Hudson Bay is a large, inland sub-Arctic sea that is isolated from open ocean circulation, and therefore acts as a relatively independent system from the Atlantic and Arctic Oceans (Stewart and Barber, 2010). Landy et al. (2017) divided the HBC into seven sub-regions. The present paper

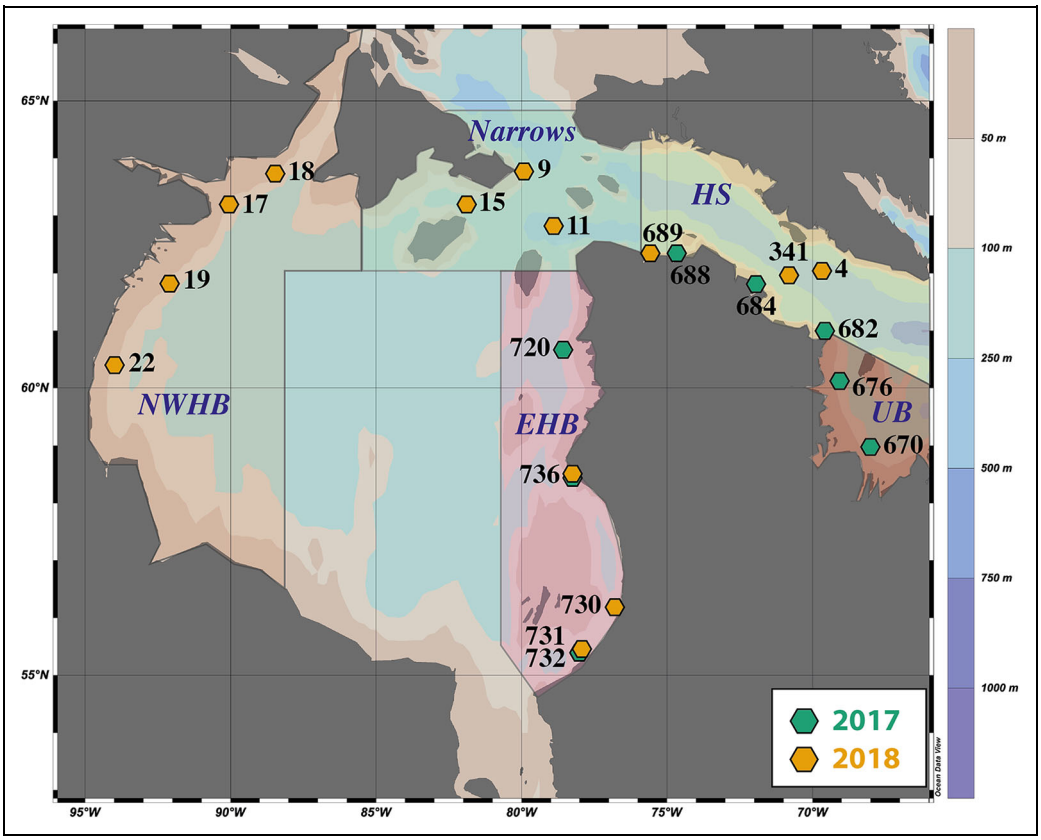

Figure 1. Map of the study area showing station locations within the Hudson Bay complex sub-regions. Stations sampled in 2017 and 2018 are indicated by green and orange hexagons, respectively, while their affiliations to the five sub-regions are outlined and shaded: Narrows Strait (Narrows), Hudson Strait (HS), Ungava Bay (UB), Eastern Hudson Bay (EHB), and Northwestern Hudson Bay (NWHB).

focuses on four of these sub-regions, i.e. Northwestern Hudson Bay (NWHB), Eastern Hudson Bay (EHB), Narrows Strait (Narrows) and Hudson Strait (HS) (**Figure 1**), as well as Ungava Bay (UB), which has been intentionally separated from its sub-region (Hudson Strait) because of its ecological and biological significance (Paulic and Rice, 2011). Water masses from the Arctic Ocean enter the HBC from the Canadian Arctic via Fury and Hecla Strait in northern Foxe Basin and from Baffin Bay via Hudson Strait (Hochheim and Barber, 2010). Within the HBC, the mostly cyclonic water circulation around the bay is eventually exported through Hudson Strait (Saucier et al., 2004; Ridenour et al., 2019). However, the major water input for the HBC is river discharge with around 760 km^3 discharged per year, more than half of which is discharged in the southern and eastern parts of the HBC (Déry et al., 2016). Furthermore, the HBC is covered by a dynamic seasonal sea ice cover from November through July (Hochheim and Barber, 2014). Due to the dominant northwesterly wind direction, sea ice breakup generally starts in the northwestern and eastern parts of Hudson Bay between May and June, and progresses toward the southern region where the last ice typically remains until late July (Andrews et al., 2018; Kirillov et al., 2020). Variability in spring ice conditions generates largely different spatial patterns in primary production between the different HBC sub-regions (Matthes et al., 2021).

2.2. Field sampling

This study was part of larger multidisciplinary investigations in the HBC aimed to understand (i) the effect of climate change on the quality of the Inuit local marine food – project BriGHT: Bridging Global Change, Inuit Health and the Transforming Arctic Ocean, as well as (ii) the contributions of climate change and hydroelectric regulation to the freshwater–marine coupling – project BaySys: The Hudson Bay System Study. Samples were collected from July 7 to 12, 2017, as part of the BriGHT project and from June 1 to July 12, 2018, as part of the BaySys project onboard the Canadian Coast Guard Icebreaker *CCGS Amundsen.* Water samples were collected with 12-L Niskin-type bottles mounted on a rosette containing a profiler that measured conductivity, temperature, and depth (CTD; SBE-911, Sea-Bird Scientific, Bellevue, WA). The rosette was also equipped with a photosynthetically active radiation sensor (PAR; scalar radiometer QSP-2300, Biospherical Instruments Inc., San Diego, CA), while a surface reference (QCR-2200, Biospherical Instruments Inc., San Diego, CA), measuring incoming scalar PAR, was mounted to the ship's main mast. Discrete water samples for nutrients, taxonomy, pigments and lipids were collected at the surface and the deep chlorophyll maximum (DCM) from bottles that were closed on the upward cast. The water was then pre-filtered using a 200-µm Nylon mesh net to remove zooplankton. Daily

fields of sea ice concentration (as % of coverage) derived from space-borne passive microwave sensors (Parkinson et al., 1996, Updated yearly) were used to calculate the number of days between sampling and the time that the site became ice-free, defined as a concentration below 15%.

2.2.1. Nutrients

Water samples for dissolved inorganic nutrients (silicate, nitrate, nitrite and phosphate) were collected into acid-washed 15-ml Falcon™ tubes after a filtration through a 25-mm Whatman GF/F filter inserted onto a filter holder to remove large particles. Nutrient concentrations were immediately measured onboard with a continuous-flow AutoAnalyzer III (Bran and Luebbe) using a routine colorimetric method adapted from Hansen et al. (1999). Analytical detection limits were 0.05 and 0.02 mmol L^{-1} for nitrate and nitrite, respectively, and 0.05 and 0.1 mmol L^{-1} for phosphate and silicate, respectively. The N:P ratio is defined here as the molar ratio of dissolved nitrogen (nitrate + nitrite) to phosphate.

2.2.2. Protist analysis

A 200-mL subsample for the identification and enumeration of eukaryotic cells >2 μm was preserved in 0.4% acidic Lugol's solution (Parsons et al., 1984) and stored in the dark at 4°C until analysis. Cells were identified to the lowest possible taxonomic rank using an inverted microscope Zeiss Axiovert 10, according to Lund et al. (1958). For each sample, a minimum of 400 cells (accuracy ± 10%) and three transects were counted at magnifications of 400×. The main taxonomic references used to identify the eukaryotic cells were Tomas (1997), Bérard-Therriault et al. (1999) and Throndsen et al. (2007).

2.2.3. Lipid analyses

Samples for lipid analyses were obtained by filtering approximately 3–5 L of seawater through Whatman GF/F glass fiber filters pre-combusted for 4 h at 450°C and stored at –80°C before further treatment at the home laboratory. An internal standard of 5$\beta\beta$-Cholanic acid (5.028 μg) was added to each sample prior to extraction. Samples were saponified (5% KOH; 90°C, 60 min; 4 mL) in a flask, then acidified with HCl to pH 1 and extracted three times with 6 mL hexane. The combined hexane extracts were dried over anhydrous Na_2SO_4, filtered and concentrated to obtain the fatty acid fraction and methylated for further detection with gas chromatography–mass spectrometry (GC-MS). GC–MS analysis of fatty acids was carried out using selected ion monitoring (SIM) mode and an Agilent 7890A series gas chromatograph (DB_{5MS} fused silica column; 50 m x 0.25 mm i.d., 0.25-μm film thickness) coupled to an Agilent 5975C mass spectrometric detector (Amiraux et al., 2020). Quantification of fatty acids was carried out by comparing mass spectral intensities of molecular ions to that of the internal standard and normalizing for volume/mass sampled and differences in mass spectral fragmentation efficiency (e.g., response factors of each fatty acids identified with Supelco® 37 Component FAME Mix, Supelco).

2.2.4. Pigment analyses

Algal pigments were determined by reverse-phase high-performance liquid chromatography (HPLC). Onboard, samples were filtered as rapidly as possible onto 25-mm Whatman GF/F filters and stored in 2-mL cryovials, wrapped in tinfoil, then flash-frozen in liquid nitrogen. Samples were stored at –80°C until analysis at the home laboratory. At the home laboratory pigments were extracted following Ras et al. (2008) and Matthes et al. (2021). Pigments and derivates were identified based on retention time and the spectral properties of external pigment standards. In this study, total chlorophyll *a* (TChl *a*) corresponds to the sum of Chl *a* and chlorophyllide *a*, total fucoxanthin corresponds to the sum of fucoxanthin, 19′-butanoyl-oxy-fucoxanthin and 19′-hexanoyl-oxy-fucoxanthin, while other carotenoids correspond to the sum of antheraxanthin, zeaxanthin and lutein. Further analyses were performed as in Galindo et al. (2017). Specifically, the ratio of photoprotective versus photosynthetic carotenoids (PPC: PSC) was calculated as the sum of PPC pigments (neoxanthin, violaxanthin, DD, alloxanthin, DT, zeaxanthin, lutein, and carotenes) versus the sum of PSC pigments (peridinin, 19′-butanoyl-oxy-fucoxanthin, fucoxanthin, 19′-hexanoyl-oxy-fucoxanthin, and prasinoxanthin). The size of the diatom xanthophyll pool (DD+DT pool) was assessed as the sum of DD and DT normalized to Tchl *a*: (DD + DT)/TChl *a*. Finally, to address the photoprotection status of phytoplankton diatoms, the DD de-epoxidation state of DD to DT was calculated as DES = (DT/[DD + DT]) × 100.

2.3. Statistical analysis

As our variables are not parametric, Mann–Whitney–Wilcoxon tests were performed to identify any significant differences between 2017 and 2018 in the environmental parameters such as temperature, salinity, PAR and dissolved inorganic nutrients affecting the phytoplankton biomass in EHB and HS. Mann–Whitney–Wilcoxon tests were also performed to identify any significant differences in carotenoid content between surface and DCM at UB and NWHB. Spearman's rank order correlation (r_s) was used to infer the strength of associations between protist classes and total fatty acids (TFA) as well as TChl *a*. Correlation significance were determined at p-value < 0.01.

To determine if the biological responses such as protist abundance, fatty acids and pigment content differed significantly between the sub-regions and depths studied, we normalised the data and performed two-way ANOVAs. Redundancy analysis (RDA; Rao, 1964) was used to identify the environmental variables (explanatory variables) influencing carotenoids and LC-PUFA content (response variables) in the different sub-regions investigated. Correlations between variables were assessed by the Spearman rank coefficient. When two variables were strongly correlated (r_s > 0.8), one was removed from subsequent analyses (Quinn and Keough, 2002). To obtain the model with the most parsimonious set of variables, a forward stepwise model selection was performed on the normalized physicochemical and biological variables (Blanchet et al., 2008). Among them, ice-free days, temperature, salinity, silicate,

diatoms, dinoflagellates, cryptophytes, choanoflagellates and prymnesiophytes were selected (dissolved nitrogen was strongly anti-correlated with dissolved silicate, and dissolved phosphate was not selected by the forward stepwise model selection). A permutation-based ANOVA was used to test the significance of axes and the term selected by the model. We performed the RDA using the "vegan" package (Oksanen et al., 2015) in R Core Team (2018).

3. Results

3.1. Environmental characteristics

The environmental parameters affecting the phytoplankton composition, abundance and content of bioactive molecules at Eastern Hudson Bay and Hudson Strait presented no significant differences between the 2017 and 2018 campaigns (Mann–Whitney–Wilcoxon, $p > 0.05$), allowing their stations from different years to be grouped together for further analysis.

At the time of sampling, the Narrows Strait sub-region (**Figure 1**) was characterized by an intact ice cover (30.0 days before it became ice-free), the lowest temperature, a high salinity, the highest concentrations in dissolved nitrogen compounds (nitrate + nitrite) and dissolved silicate, as well as the highest N:P ratio (**Table 1**). Stations defining our Hudson Strait sub-regions were close to becoming ice-free at the time of sampling (4.4 days in advance) and presented relatively low nutrient concentrations at the surface compared to DCM. The stations defining Ungava Bay presented relatively similar high temperature and salinity conditions to those of Hudson Strait, while Ungava Bay had been ice-free for a longer period before sampling (11.3 ice-free days) and presented a more pronounced nutrient surface depletion than Hudson Strait (**Table 1**). The Eastern Hudson Bay sub-region was defined by the longest period of ice-free days prior to sampling (15.5 days), the lowest salinity and the highest temperature, as well as low dissolved nitrogen compounds and high dissolved phosphate concentrations (**Table 1**). Finally, the stations defining the Northwestern Hudson Bay (**Figure 1**) were mostly ice-free (ice-free for 3.8 days prior to sampling) and low in dissolved nitrogen compounds, as well as in phosphate (**Table 1**).

3.2. Protist composition, TChl a and total lipid content

Although the composition of protists differed significantly between the regions and depths investigated, their total abundance did not differ (**Figure 2**; Table S1). The mean ($\pm$ SE) abundance of protists across the different sub-regions and depths was $1.08 \pm 0.12 \times 10^6$ cells L^{-1} (**Figure 2**). In terms of relative composition, surface and DCM samples overall were dominated by unclassified flagellates (44.9 and 38.1%, respectively), diatoms (pennate and centric; 30.3 and 44.4%, respectively), and choanoflagellates (10.2 and 6.3%, respectively; **Figure 2**). TChl *a* content differed significantly between sub-regions with content ranging from 0.3 to 2.8 μg L^{-1}, as well as between sampling depths, although the latter difference originated mainly from the HS sub-region (**Figure 3A**; Table S1). TFA content did not differ significantly between sampling depths, while it differed significantly between sub-regions, with content ranging from 7.6 to 88.6 μg L^{-1} (**Figure 3B**; Table S1). Surface diatom abundance did not correlate with TChl *a,* while it correlated strongly with TFA (Spearman's $r_s = 0.38$, $p > 0.05$, and $r_s = 0.75$, $p < 0.001$, respectively). At the DCM, diatom abundance correlated strongly with both TChl *a* and TFA content (Spearman's $r_s > 0.78$, $p < 0.001$).

At the time of sampling, the Narrows sub-region was defined by a similar protist composition, TChl *a* and TFA content at the surface and at the DCM (**Figures 2** and **3**). This sub-region was characterized by the highest dominance of unclassified flagellates with approximately 65% associated with the lowest contents of TChl *a* and TFA (mean of 0.4 and 11.0 μg L^{-1}, respectively).

The HS sub-region was characterized by a slight increase in diatoms and unclassified flagellates with depth, which was associated with a doubling of Tchl *a* from 1.4 to 2.8 μg L^{-1} (**Figures 2** and **3A**). However, TFA contents were not significantly different between depths, with 54.5 and 64.9 μg L^{-1} at the surface and DCM, respectively (**Figure 3B**).

The UB sub-region was defined by a similar protist composition, TChl *a* and TFA content at the surface and DCM. This sub-region was defined by the highest dominance of diatoms of approximately 84%, which was associated with the highest TFA contents and high TChl *a* (**Figures 2** and **3)**. TFA content at UB was above 61.4 μg L^{-1}, while TChl *a* mean was at 1.9 μg L^{-1} at both depths.

The EHB sub-region presented a notable difference in protist composition between the surface and DCM. The surface layer was dominated at 55.6% by unclassified flagellates, while the DCM was dominated at 70.5% by diatoms. The EHB protist composition also showed the highest contribution of dinoflagellates at 15%, mainly represented by *Heterocapsa rotundata* at the surface (**Figure 2**). TChl *a* and TFA contents were not significantly different between depths, with mean of 2.5 and 30.5 μg L^{-1}, respectively (**Figure 3**).

The NWHB sub-region was dominated by unclassified flagellates and was characterised by the largest contribution of choanoflagellates. The latter represented 33.2 and 21.6% of the protist community at the surface and DCM, respectively (**Figure 2**). TChl *a* and TFA contents were not significantly different between depths, with mean of 1.6 and 33.6 μg L^{-1}, respectively (**Figure 3**).

3.3. Fatty acid content and composition

The lipid profiles of samples from all sub-regions consisted of saturated (SFA), monounsaturated (MUFA) and polyunsaturated fatty acids (PUFA; **Figure 4**). Only fatty acids with a contribution >1% are represented in **Figure 4**. SFA were composed of $C_{14:0}$ myristic acid, $C_{16:0}$ palmitic acid and $C_{18:0}$ stearic acid. MUFA were composed of $C_{16:1\ n\text{-}7}$ palmitoleic acid, $C_{18:1n\text{-}9\ cis}$ oleic acid and $C_{18:1n\text{-}9\ trans}$ elaidic acid. PUFA were composed of $C_{18:2\ n\text{-}6}$ linoleic acid (LA), $C_{18:3\ n\text{-}3}$ α-linolenic (ALA), $C_{18:3\ n\text{-}6}$ γ-linolenic acid (GLA), $C_{20:5\ n\text{-}3}$ eicosapentaenoic acid (EPA) and $C_{22:6\ n\text{-}6}$ docosahexaenoic acid (DHA). The mean relative contribution of SFA, MUFA and PUFA was 24.8%,

Table 1. Environmental data (mean ± standard error) for the surface and deep chlorophyll maximum (DCM) of the five investigated sub-regions of the Hudson Bay complex (Figure 1)

Region	Date (mm/dd)	Ice Free (days)[a]	Layer	Depth (m)	n	PAR (μmol Photons s^{-1} m^{-2})	Temperature (°C)	Salinity	Nitrate + Nitrite (μmol L^{-1})	Phosphate (μmol L^{-1})	Silicate (μmol L^{-1})	N:P (molar)
Narrows	06/04 ± 1.0	−30.00 ± 1.70	Surface	0	3	52.51 ± 1.23	−1.49 ± 0.08	31.66 ± 0.43	4.06 ± 0.41	0.89 ± 0.02	10.52 ± 0.48	4.56 ± 0.37
			DCM	27.5 ± 1.9	3	0.47 ± 0.10	−1.55 ± 0.08	31.78 ± 0.44	5.97 ± 0.73	0.91 ± 0.04	11.19 ± 0.64	4.92 ± 0.58
HS	07/03 ± 8.0	4.4 ± 8.93	Surface	0	5	644.0 ± 231.4	1.42 ± 0.91	31.26 ± 0.59	0.98 ± 0.91	1.16 ± 0.76	1.91 ± 1.22	1.40 ± 1.21
			DCM	21.2 ± 2.3	5	5.28 ± 2.54	−0.66 ± 0.39	31.94 ± 0.37	2.45 ± 0.80	2.13 ± 1.03	2.74 ± 1.07	2.66 ± 1.30
UB	07/11 ± 0.3	11.33 ± 1.12	Surface	0	3	758.4 ± 378.2	1.62 ± 1.08	30.66 ± 0.53	0.05 ± 0.05	0.32 ± 0.04	0.42 ± 0.28	0.13 ± 0.12
			DCM	33.0 ± 3.0	3	1.6 ± 1.19	−0.41 ± 0.27	31.49 ± 0.09	1.2 ± 0.52	0.51 ± 0.09	1.81 ± 0.89	2.08 ± 0.78
EHB	07/08 ± 0.3	15.5 ± 6.63	Surface	0	6	700.2 ± 179.3	4.75 ± 1.14	26.29 ± 0.97	0.11 ± 0.06	4.79 ± 2.14	2.26 ± 1.17	0.09 ± 0.05
			DCM	33.8 ± 4.7	6	0.29 ± 0.22	−0.15 ± 0.72	28.42 ± 1.00	1.75 ± 0.48	7.10 ± 2.84	4.69 ± 1.85	0.96 ± 0.55
NWHB	06/08 ± 0.85	3.75 ± 8.10	Surface	0	4	734.7 ± 276.6	−0.05 ± 0.52	32.31 ± 0.22	0.16 ± 0.57	0.57 ± 0.03	2.71 ± 1.53	0.25 ± 0.20
			DCM	27.0 ± 5.6	4	11.43 ± 9.17	−1.08 ± 0.06	32.71 ± 0.21	0.47 ± 0.39	0.59 ± 0.09	3.12 ± 1.81	0.70 ± 0.49

[a]Number of days the station had been ice-free at the time of sampling.

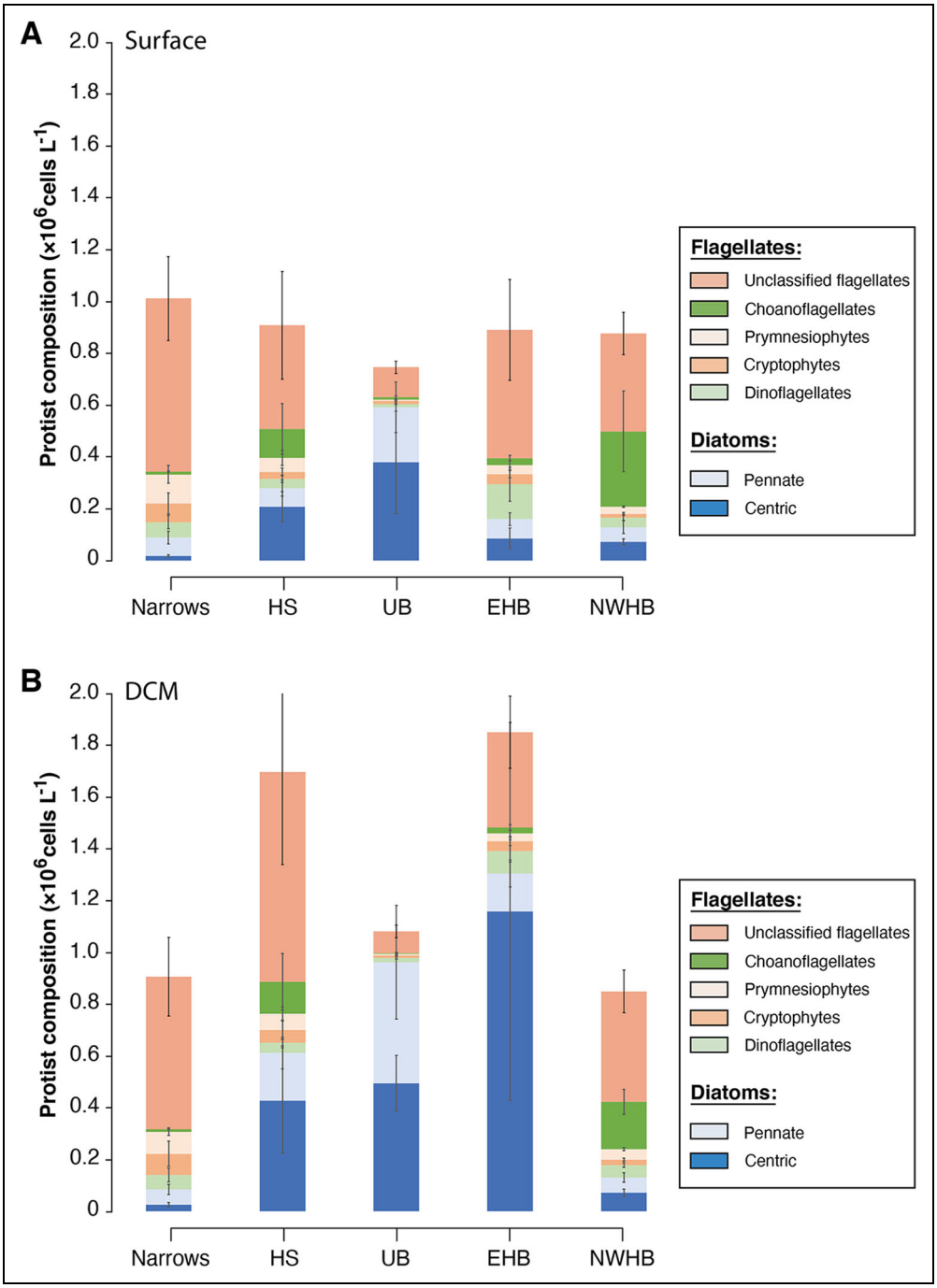

Figure 2. Protist community composition in the Hudson Bay complex. Microalgal community composition ($\times$ 10^6 cells L^{-1}), determined by microscopic analysis, for the (A) surface and (B) deep chlorophyll maximum (DCM) of the five Hudson Bay complex sub-regions: Narrows Strait (Narrows), Hudson Strait (HS), Ungava Bay (UB), Eastern Hudson Bay (EHB), and Northwestern Hudson Bay (NWHB; **Figure 1**). Error bars indicate standard error.

40.6% and 34.6%, respectively, and the fatty acid profiles were dominated by palmitoleic acid, EPA, palmitic acid and DHA at 29.6, 21.0, 13.3 and 10.5%, respectively.

SFA, MUFA and PUFA differed significantly between sub-regions but not between depths. However, some of the fatty acids constituting these lipid classes differed significantly between sub-regions and depths (**Figure 2**; Table S1).

The Narrows exhibited the lowest TFA content, which was associated with the highest SFA contribution at the detriment of PUFA (**Figure 4**). HS and UB sub-regions exhibited the highest TFA content associated with the highest PUFA contribution and the lowest SFA content (**Figure 4**). In EHB, the TFA content exhibited a slightly higher SFA contribution at the detriment of PUFA compared to what was observed in the other sub-regions (**Figure 4**). However, the surface was characterized by the highest DHA and ALA contribution to the total fatty acids at 13.2 and 1.7%, respectively, while at the DCM these PUFA contributed similarly to what was observed in the other sub-regions. In NWHB, the TFA content exhibited

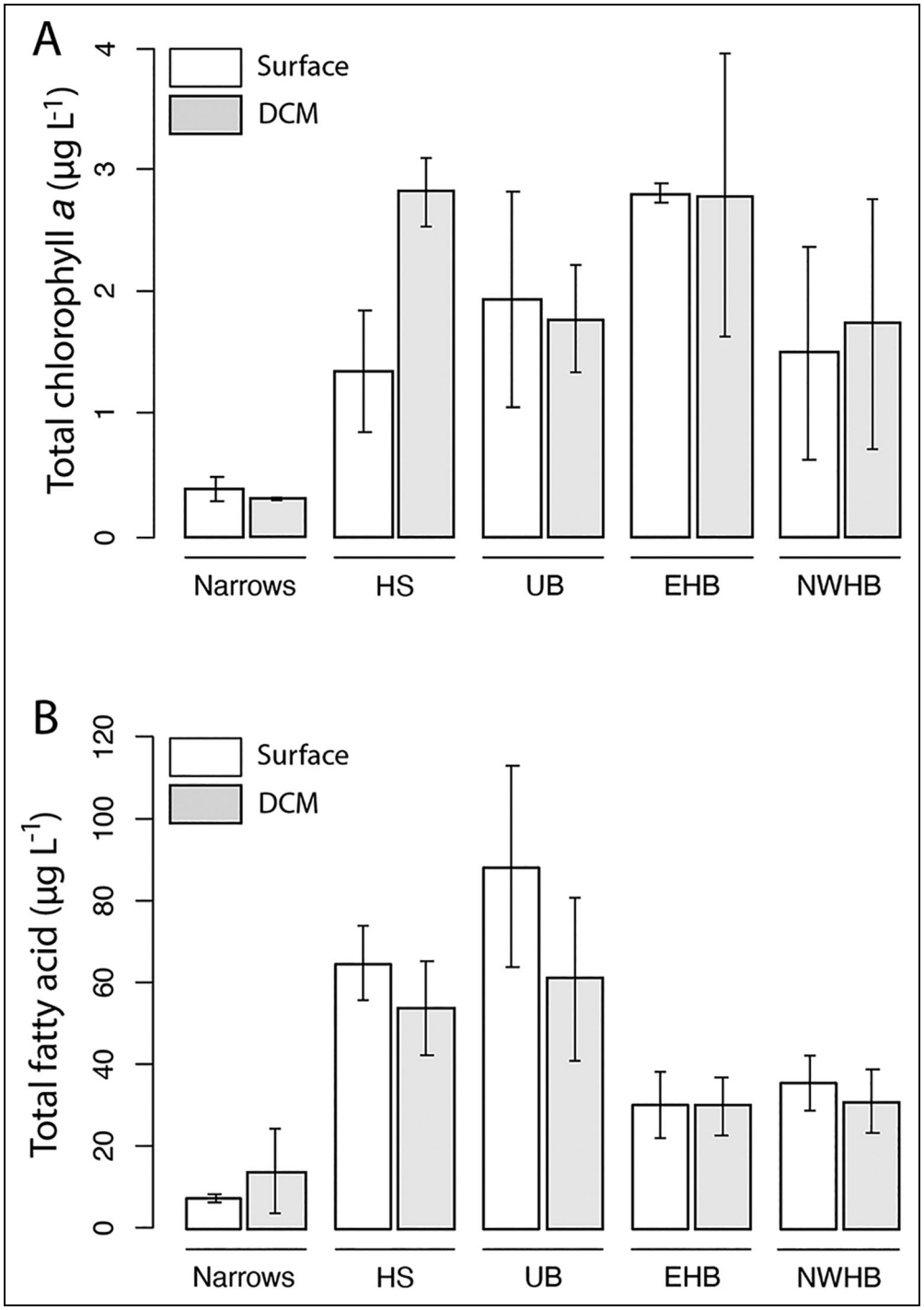

Figure 3. Total chlorophyll *a* and total fatty acids in the Hudson Bay complex. (A) Total chlorophyll *a* (µg L^{-1}) and (B) total fatty acids (µg L^{-1}) observed at the surface (white bars) and at the deep chlorophyll maximum (DCM; gray bars) of the five Hudson Bay complex sub-regions investigated: Narrows Strait (Narrows), Hudson Strait (HS), Ungava Bay (UB), Eastern Hudson Bay (EHB), and Northwestern Hudson Bay (NWHB; **Figure 1**). Error bars indicate standard error.

a slightly higher MUFA contribution at the detriment of PUFA than the average contributions for all sub-regions (**Figure 4**).

3.4. Pigment content and composition

Many carotenoids and chlorophylls were identified (Figure S1). Carotenoids included prasinoxanthin, neoxanthin, peridinin, fucoxanthin, β-carotene, violaxanthin, DD, DT and alloxanthin, while chlorophylls included chlorophyll *a*, *b*, *c*, phaeophytin *a*, phaeophorbide *a* and chlorophyllide *a*. The pigment content of samples was dominated by chlorophyll *a*, as well as fucoxanthin and its derivatives at 58.5 and 23.9%, respectively (Figure S1). Among carotenoids, fucoxanthin and derivatives, DD+DT and β-carotene dominated at 86.8, 5.4 and 3.1%, respectively. Absolute carotenoid concentration at the surface was

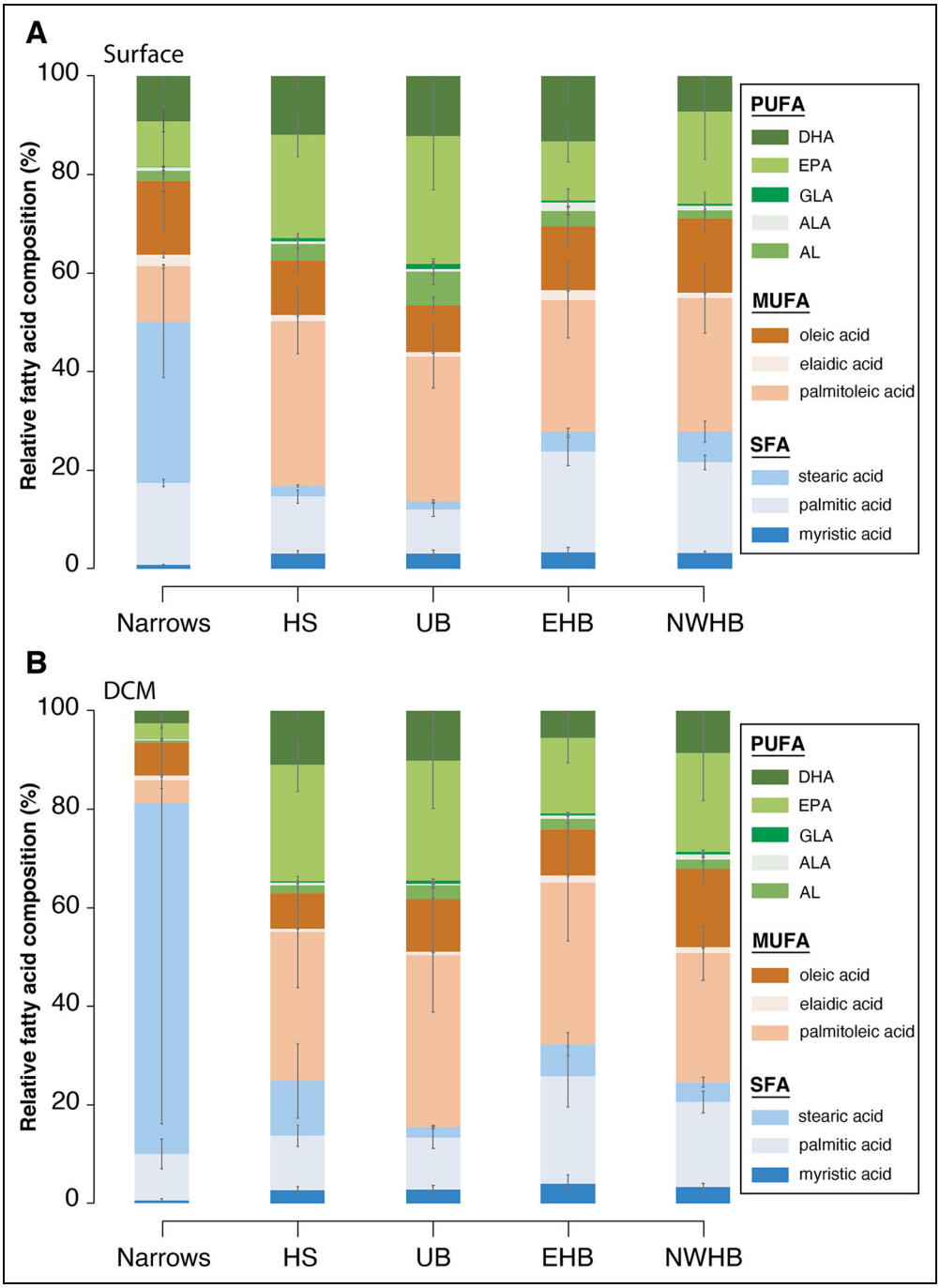

Figure 4. Relative fatty acid composition in the Hudson Bay complex. Relative fatty acid composition (% of total fatty acids) for polyunsaturated (PUFA), monounsaturated (MUFA) and saturated fatty acids (SFA) at the (A) surface and (B) deep chlorophyll maximum (DCM) of the five Hudson Bay complex sub-regions investigated: Narrows Strait (Narrows), Hudson Strait (HS), Ungava Bay (UB), Eastern Hudson Bay (EHB), and Northwestern Hudson Bay (NWHB; **Figure 1**). Error bars indicate standard error.

almost half the value at the DCM, with 0.51 and 0.89 μg L^{-1}, respectively.

The Narrows samples showed almost no carotenoids (**Figures 5** and S1). The carotenoid content of HS surface samples was less than half than at the DCM, while in UB, surface and DCM carotenoid contents and relative contributions were not significantly different (Mann–Whitney–Wilcoxon, $p > 0.05$). EHB differed from other sub-regions because its surface samples exhibited the highest absolute concentrations of prasinoxanthin, neoxanthin and peridinin, while the relative contribution of these pigments was diminished by the strong relative fucoxanthin contribution at the DCM. Although the surface samples of EHB had some of the lowest carotenoid contents, the DCM samples had the highest content (**Figure 5**). The NWHB surface and DCM carotenoid contents were not significantly different (Mann–Whitney–Wilcoxon, $p > 0.05$), with a content almost exclusively comprised of fucoxanthin

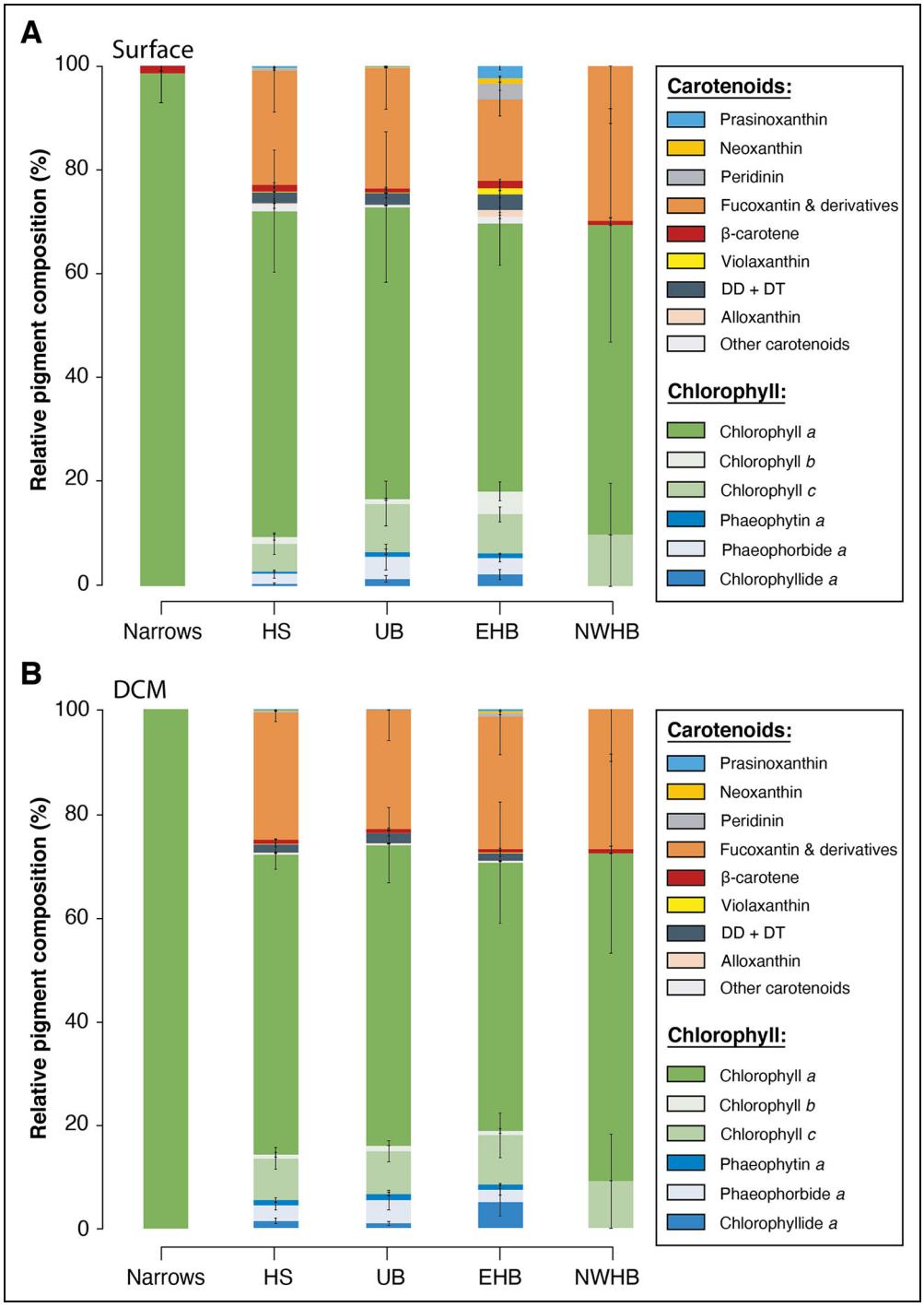

Figure 5. Relative carotenoid and chlorophyll concentrations in the Hudson Bay complex. Relative carotenoid and chlorophyll composition (% of total pigments) at the (A) surface and (B) deep chlorophyll maximum (DCM) of the five Hudson Bay complex sub-regions investigated: Narrows Strait (Narrows), Hudson Strait (HS), Ungava Bay (UB), Eastern Hudson Bay (EHB), and Northwestern Hudson Bay (NWHB; **Figure 1**). Error bars indicate standard error.

(approximately 97% of carotenoids, 0.75 µg L^{-1}; **Figures 5** and S1).

As expected from the large differences in underwater PAR levels (**Table 1**), the PPC: PSC ratio was higher at surface than at DCM, independent of the sub-regions considered (**Figure 6**). While PAR was relatively steady at DCM, it showed marked differences at surface with highest values in the EHB and NWHB sub-regions as compared to the Narrows, HS and UB sub-regions. When focusing on the photoprotective pigments specific to diatoms: DD and DT (Figure S2), a similar surface versus DCM pattern was observed, i.e. the DD+DT pool size, as well as the DES, were higher at surface than at DCM. Independent of depth, Hudson Bay stations (EHB) and stations outside of Hudson Bay (HS) showed the same DD+DT pool size. This similarity was in relative contrast to surface PPC: PSC ratios, which were higher in EHB waters, suggesting the significant presence of non-diatom photoprotective

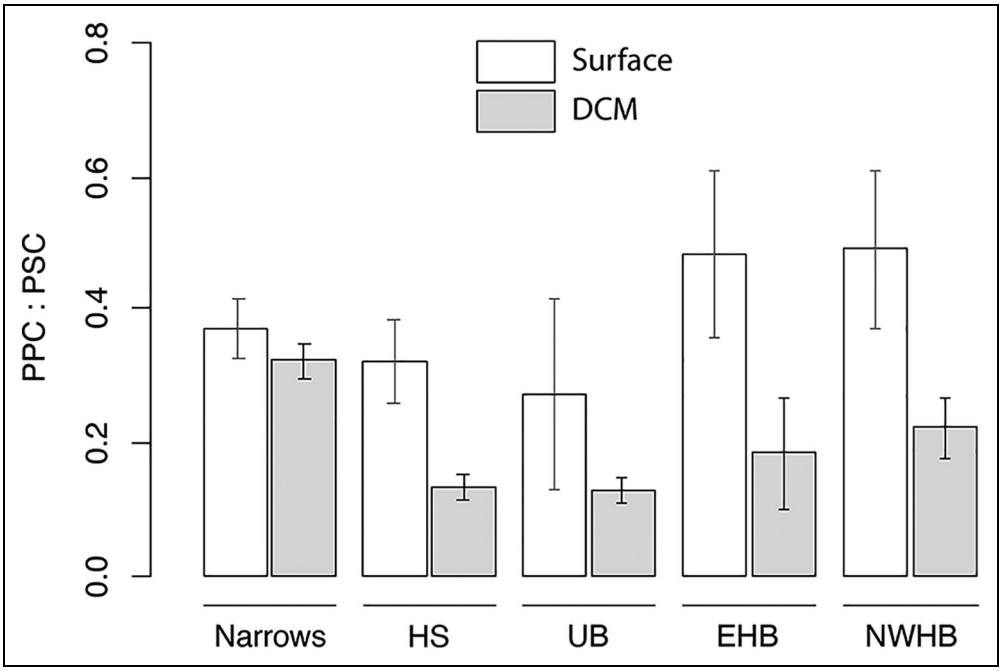

Figure 6. Photoprotective to photosynthetic carotenoids (PPC: PSC) in the Hudson Bay complex. PPC: PSC ratio at the surface (white bars) and deep chlorophyll maximum (DCM; gray bars) of the five sub-regions investigated in the Hudson Bay complex: Narrows Strait (Narrows), Hudson Strait (HS), Ungava Bay (UB), Eastern Hudson Bay (EHB), and Northwestern Hudson Bay (NWHB; **Figure 1**). Error bars indicate standard error.

pigments. While DES at the DCM was similar for both sub-regions, it was double in HS waters (i.e., 20.3 versus 11.9%) due to the highest concentration of DT.

3.5. Environmental drivers of fatty acid and carotenoid contents

The RDA model explained 46% ($r^2_{adj.} = 0.47$) of the total multivariate fatty acid and carotenoid variation (**Figure 7**). Diatoms, high numbers of ice-free days and low dissolved silicate concentrations were associated with most LC-PUFA (EPA, DHA, GLA, LA) and carotenoids (fucoxanthin and derivatives, β-carotene, DD+DT; **Figure 7**). Stations with these conditions were located mainly in the UB and HS sub-regions, while the stations with the opposite conditions (i.e., choanoflagellates, high dissolved silicate and low numbers of ice-free days) belong to the NHWB and Narrows sub-regions. Dinoflagellates, high temperature and low salinity were associated with minor LC-PUFA (ALA) and carotenoids (peridinin, violaxanthin, neoxanthin, prasinoxanthin, alloxanthin and other carotenoids). The stations with these conditions were located mainly in the EHB sub-region.

4. Discussion

In spring, the changes in environmental factors such as light, sea ice cover, temperature and salinity control the phenology of the protist communities, their bloom stages and, consequently, the water content of bioactive molecules (Lee and Whitledge, 2005; Leu et al., 2006; Popova et al., 2010; Coupel et al., 2015; Tremblay et al., 2015; Ardyna et al., 2020). The different sub-regions investigated in this study presented contrasting environmental conditions that favoured different stages of the spring phytoplankton bloom: pre-bloom (Narrows), surface bloom (HS), deepening bloom (UB) and post-bloom (NWHB; **Figure 8**). Pre-bloom stage was characterized by a protist community dominated by flagellates. This community biosynthesizes low contents of LC-PUFA and carotenoids and, consequently, the content of bioactive molecules was low (**Figure 9**). During the surface bloom and subsequent deepening, the environmental conditions favoured a diatom-dominated protist community. Diatoms are known to be a productive source of the main LC-PUFA and carotenoids (Viso and Marty, 1993; Kelly and Scheibling, 2012; Kuczynska et al., 2015), which supports the high content of these bioactive molecules observed during their bloom. Post-bloom stage is characterized by a dominance of flagellates, including a strong contribution of choanoflagellates. The latter biosynthesize low quantities of LC-PUFA and carotenoids, and the contents observed in bioactive molecules at this stage of bloom most likely derived from the less abundant diatoms. We conclude that the availability of bioactive molecules, LC-PUFA and carotenoids, in the HBC originates mainly from diatoms, especially when they dominate the protist community during the phytoplankton bloom (**Figures 2** and **9**). Our study also described a bloom-deepening scenario due to riverine inputs (EHB area). This scenario showed a different protist community than the purely marine scenario, with a particularly high abundance of mesohaline dinoflagellates (*Heterocapsa rotundata*). This scenario showed a specific, albeit low, bioactive molecule content, with LC-PUFA and carotenoids that differed from those reported for the other bloom stages (**Figure 9**). As both diatom- and dinoflagellate-dominated blooms are typical features of marine and brackish waters, respectively (Ardyna et al.,

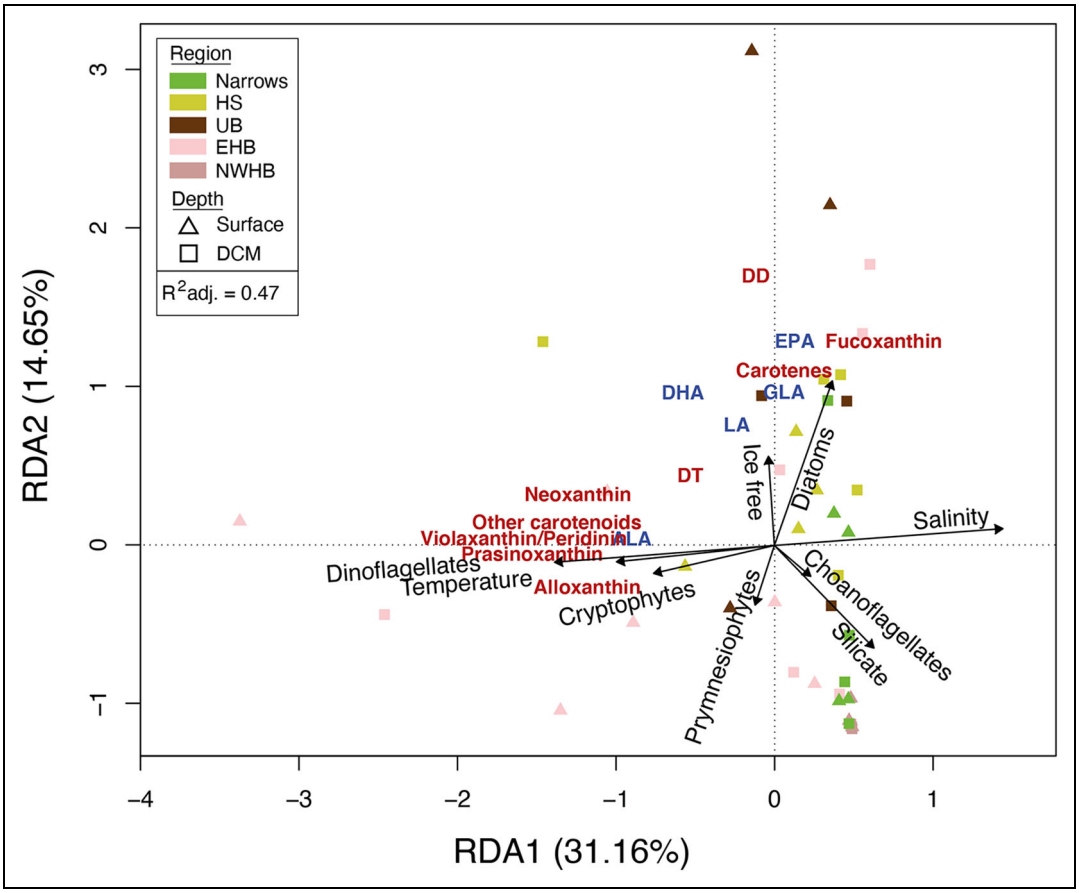

Figure 7. Redundancy analysis of environmental variables best explaining variation in bioactive molecules at the study sites. Plot of the redundancy analysis (RDA) models. By selecting (forward stepwise model selection) ice-free days, temperature, salinity, dissolved silicate, diatoms, choanoflagellates, dinoflagellates, cryptophytes, and prymnesiophytes as variables, the RDA model explained 46% ($r^2_{adj.}$= 0.47) of the total multivariate fatty acid and carotenoid variation. Color-coded sub-regions investigated in the Hudson Bay complex are: Narrows Strait (Narrows), Hudson Strait (HS), Ungava Bay (UB), Eastern Hudson Bay (EHB), and Northwestern Hudson Bay (NWHB; **Figure 1**).

2017; Krause et al., 2019), the scenarios we observed in this study may represent the general phenology in most of the Arctic and sub-Arctic regions.

4.1. Spring phytoplankton bloom scenarios in the HBC and associated bioactive molecules

The pre-bloom scenario observed at Narrows was distinguished from the others mainly by the presence of sea ice, higher nutrient concentrations, lower TChl *a* and total fatty acid content, and a strong dominance of unclassified flagellates (**Figures 8** and **9**). The low carotenoid and LC-PUFA contents are explained in our RDA model by typical pre-bloom physico-chemical conditions, i.e. a high seawater dissolved silicate concentration and an intact sea ice cover (**Figure 7**). Diatoms are the dominant contributors to Arctic Ocean spring blooms (Wassmann et al., 1999; Vaquer-Sunyer et al., 2013; Krause et al., 2018), and their productivity depends on the availability of dissolved silicate which they use to build their silica shells (Krause et al., 2018). Moreover, diatoms are the main producers of the major LC-PUFA EPA, as well as of the major carotenoids fucoxanthin, DD and DT (Viso and Marty, 1993; Kelly and Scheibling, 2012; Kuczynska et al., 2015). Thus, the pre-blooming scenario, which is characterized by the lowest presence of diatoms, results in the lowest content of LC-PUFA and carotenoids (**Figure 9**).

The surface bloom scenario observed at HS was characterized by a recent disappearance of sea ice, high nutrient availability throughout the water column and high algal biomass and fatty acid content that was associated with a co-dominance of diatoms and unclassified flagellates. Of this scenario, the deepening bloom scenario observed at UB was distinguished by a longer ice-free period, the disappearance of surface nutrients as well as an increased lipid content that was associated with a strong dominance of diatoms. In our RDA model (**Figure 7**), the particularly high contents of LC-PUFA and carotenoids during the surface bloom and its deepening were explained by the dissolved silicate draw-down associated with open water conditions, indicating a diatom-dominated marginal ice zone bloom. Consequently, we observed the highest contents in diatom-related LC-PUFA EPA and the carotenoids fucoxanthin, DD and DT, although other molecules less specific to diatoms and in lower abundance were also present, and possibly synthesized in part by flagellates, i.e. DHA, GLA, LA and β-carotene (**Figures 4**, **5**, **7**, S1, and S2). Our hypothesis is that

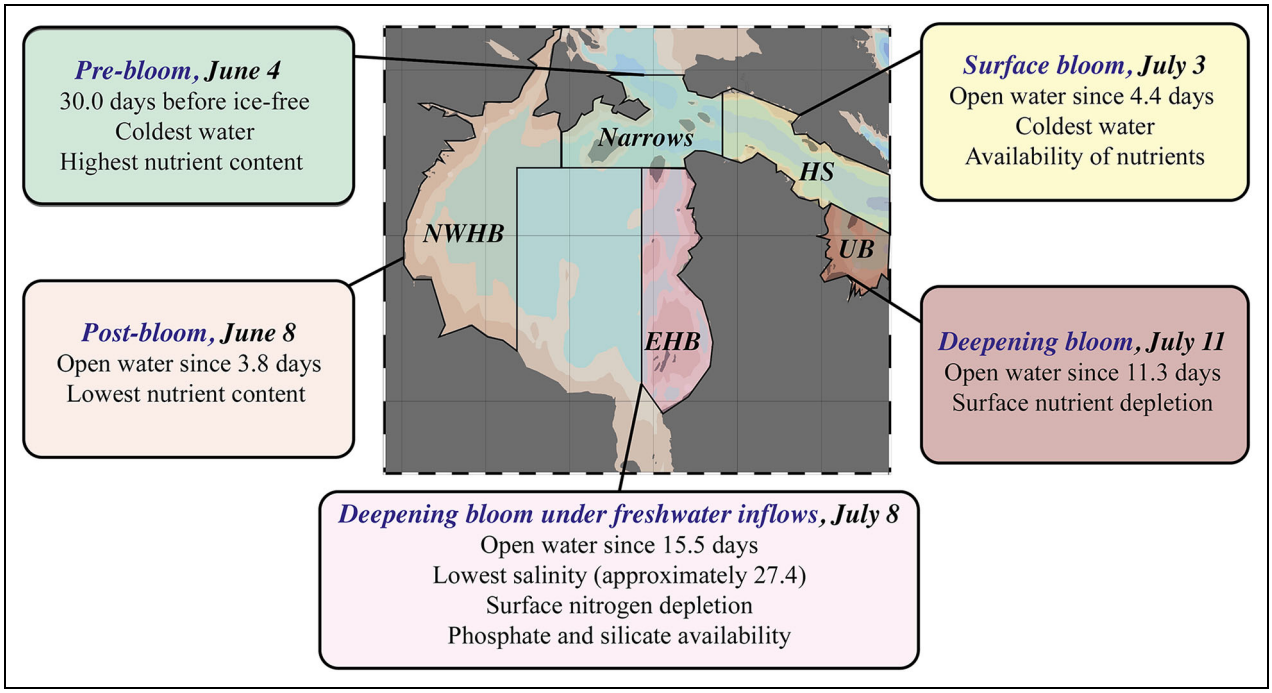

Figure 8. Schematic summarizing the major environmental characteristics that conditioned blooming stages in the Hudson Bay complex. Environmental characteristics (date, ice condition, salinity, temperature and nutrient) that conditioned the different bloom stages in the five sub-regions investigated in the Hudson Bay complex: Narrows Strait (Narrows), Hudson Strait (HS), Ungava Bay (UB), Eastern Hudson Bay (EHB), and Northwestern Hudson Bay (NWHB; **Figure 1**).

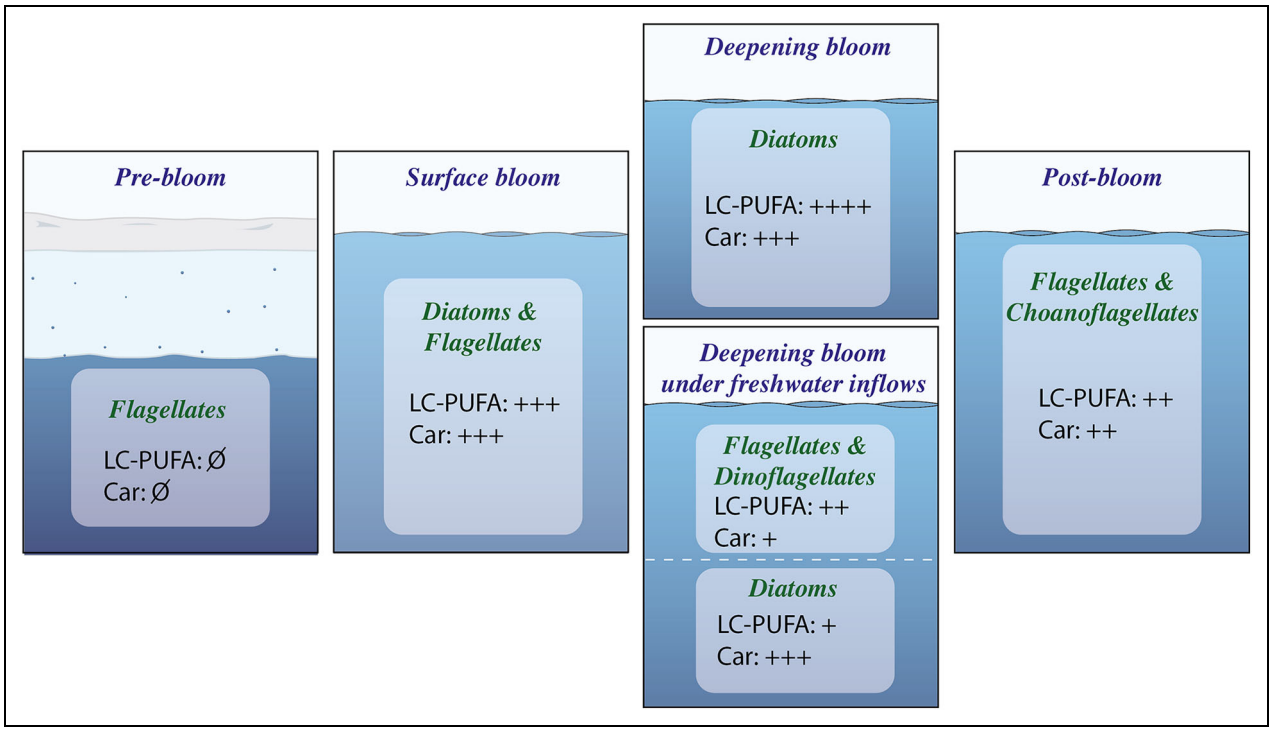

Figure 9. Schematic summarizing the phenology and bioactive molecule content of protists during the blooming stages. Long-chain polyunsaturated fatty acid (LC-PUFA) and carotenoid (Car) content during the five bloom stages observed in the Hudson Bay complex: pre-bloom, surface bloom, deepening bloom, deepening bloom under freshwater inflows, and post-bloom. The gradient in this content is depicted from absent (Ø) to low (+), moderately low (++), moderately high (+++) and high (++++) content.

diatoms are so productive during the surface and deepening bloom that their production of minor LC-PUFA is greater than that of genera that produce them in significant quantities (Dunstan et al., 1994). Therefore, we suggest that LC-PUFA and carotenoids are mostly provided by diatoms during the spring bloom. Interestingly, Leu et al. (2006) showed in High Arctic fjord waters that during the surface bloom scenario, well before the maximum algal biomass, the maximum contribution of LC-PUFA to total fatty acids was reached and accounted for approximately 45%. In the present paper, the maximum contribution of LC-PUFA to total fatty acids of approximately 42% was observed in the deepening bloom scenario, although it had probably reached a biomass peak, as evidenced by the high TChl *a* content associated with a lack of nutrients (**Table 1**, **Figure 3A**).

The riverine input-forcing bloom-deepening scenario observed in EHB differed from the UB deepening bloom scenario mostly by its surface layer content. In EHB, the very low salinity and warm temperatures at surface (26.29 and 4.75°C, respectively) favoured the dominance of unclassified flagellates (**Figures 8** and **9**). In our RDA model (**Figure 7**), the surface low salinity and warm temperatures coincide with the highest content in peridinin, violaxanthin, neoxanthin, prasinoxanthin and alloxanthin carotenoids, which is explained by the higher protist diversity. For instance, peridinin and alloxanthin are respectively synthesized by dinoflagellates and cryptophytes (Johansen et al., 1974; Thomson et al., 2004; Šupraha et al., 2014), which were the most abundant carotenoids in this scenario compared to the others. Interestingly, our RDA model also highlights that the riverine input-forcing bloom-deepening scenario enhances the content of ALA LC-PUFA in surface waters. EHB DCM waters presented the typical characteristic of a deepening diatom-dominated bloom, namely a strong content of LC-PUFA and carotenoids, as observed in HS (**Figures 8** and **9**).

The post-bloom scenario observed in NWHB was characterized by strong nutrient depletion throughout the water column, suggesting that the bloom-deepening scenario had already occurred. A further sign of stressful growth conditions at surface was the highest PPC: PSC ratio observed (**Figure 6**; Matthes et al., 2021). The post-bloom scenario showed low carotenoid and LC-PUFA water contents that were explained in our RDA model by high seawater dissolved silicate and a strong contribution of choanoflagellates to the protist community (**Figure 7**). The lack of nutrients (except silicate) and the dominance of choanoflagellates indicate a food web functioning based on the microbial loop, which is characteristic for the post-bloom stage (McKenzie et al., 1997; Thaler and Lovejoy, 2015). As choanoflagellates are unpigmented (Brunet et al., 2019), the observed carotenoid pattern (high fucoxanthin) likely originated from the non-dominant diatoms (see our hypothesis above). Similarly, the LC-PUFA EPA contents also likely originated from diatoms, even if non-dominant (**Figures 8** and **9**).

4.2. Potential impact of climate warming on the production of bioactive molecules in the HBC

In this study, we focused on the HBC because it is one of the Arctic regions most affected by global warming in terms of increasing temperatures and freshwater supplies. Such changes in environmental conditions are expected to alter the production of bioactive molecules by microalgae at the basis of the food web, and thus modify the dynamics of the marine ecosystem on which the indigenous communities living on its shores depend.

As a consequence of global warming, primary production increased by 57% between 1998 and 2018 in the Arctic Ocean (Lewis et al., 2020). Although an increase in light, due to the melting of snow and ice cover, is generally considered to be the main driver of phytoplankton production, over the last decade the increase in phytoplankton biomass may instead have been supported by an influx of new nutrients. The HBC upper water column is vertically stable perennially mainly due to buoyancy forces associated with freshwater inputs from numerous large rivers and the seasonal ice melt cycle (Prinsenberg, 1986). This haline stratification restricts upward nutrient flux to the surface layer (Ingram and Prinsenberg, 1998). Although the future contribution of wind patterns to vertical mixing remains uncertain, one of the expected consequences of global warming in the HBC is stronger water column stratification. These conditions should benefit small protist cells, as they are more efficient in acquiring nutrients and less susceptible to gravitational sedimentation than larger and/or heavy cells, such as diatoms (Li et al., 2009). As a consequence, stronger prevalence of a flagellate-based food web in the HBC, at the detriment of a diatom-based food web, is expected (Li et al., 2009; Lalande et al., 2013; Nöthig et al., 2015). The decrease in the contribution of diatoms to the protist community should thus lead to a reduction in the availability of the main bioactive molecules they produce, i.e. EPA LC-PUFA and fucoxanthin, DD and DT carotenoids.

In coastal regions influenced by rivers, climate warming is expected to result in increasing riverine inflows. These features should reinforce the already established stratification, but more importantly increase nutrient availability (Terhaar et al., 2021). The magnitude of protist blooms that develop in these transition zones, and that we observed in the riverine input-forcing scenario, should increase. A future increase in the availability of minor bioactive molecules in coastal HBC areas, such as ALA LC-PUFA and peridinin, violaxanthin, neoxanthin, prasinoxanthin and alloxanthin carotenoids, is therefore expected. In addition to an expected shift from high- to low-producing protist communities, higher temperatures are expected to alter LC-PUFA biosynthesis. Protists adapt to changing temperatures by modifying the structure of their membranes, a process known as homeoviscous adaptation (Sinensky, 1974; Winter and Dzwolak, 2005; D'Amico et al., 2006). This process involves the remodeling of membrane lipids by modifying fatty acid chain length and unsaturation to maintain the desired level of fluidity of cell membranes (Guschina and Harwood, 2006). The double bonds in LC-PUFA enhance the ability of fatty acids to 'bend', which increases flexibility and leads to increased membrane fluidity in cold

environments. In turn, protists reduce membrane LC-PUFA content in response to increasing temperatures in order to maintain cell membrane structural rigidity in a less ordered environment (Rousch et al., 2003; Fuschino et al., 2011). An increase in water temperature by 2.5°C has been estimated to lead to a LC-PUFA synthesis reduction by 8.2% for EPA and 27.8% for DHA (Hixson and Arts, 2016). In addition to rising temperatures, other environmental conditions related to climate change, such as ocean acidification (Duncan et al., 2022) and changes in light intensity (Piepho et al., 2012), may also affect LC-PUFA availability and to a larger extent the nutritional value of phytoplankton. Decreased sea ice thickness, less snow cover, an earlier ice breakup and the reinforcement of stratification result in higher ambient irradiances during spring phytoplankton blooms (Strom and Fredrickson, 2008; Nicolaus et al., 2012). Although higher light availability may boost the annual marine primary production, some studies have highlighted a lower LC-PUFA biosynthesis due to light stress (Leu et al., 2010; Leu et al., 2016).

5. Conclusions

At the time of sampling, the HBC sub-regions studied were in different bloom stages that reflected the physico-chemical characteristics of their waters. Pre- and post-bloom stages were associated with a dominance of flagellates that presented low contents of bioactive molecules, while the surface and deepening bloom stages were associated with a dominance of diatoms, efficient producers of major LC-PUFA and carotenoid pigments. The highest concentrations of bioactive molecules were associated with the diatom bloom and/or dominance. These observations further confirm the crucial importance of diatoms in determining the nutritional quality of the food web within the HBC and the Arctic Ocean. However, climate change threatens the future availability of these bioactive molecules because of the concomitant expected decreasing dominance of diatoms in Arctic marine primary production, increasing light and temperature, and other climate change impacts such as ocean acidification. Consequently, a potentially profound alteration of the food web functioning and, more broadly, of the dynamics of the Arctic marine ecosystem is to be expected.

Our study also identified the effects of riverine inputs, which are increasing with global warming, on the production of phytoplankton bioactive molecules. The riverine inputs observed in the EHB sub-region and identified by the low surface salinities led to a diversification of the protist community with a strong presence of the mesohaline dinoflagellates *Heterocapsa rotundata*. This peculiar protist community presented a relatively low yet diverse content of bioactive molecules, with the highest contribution of DHA and peridinin. The expected future increase in freshwater inputs into the HBC and more broadly the Arctic basins, will most likely lead to an increase in the availability of minor bioactive molecules. However, this 'new' production is not expected to counterbalance the possibly dramatic losses of diatom-sourced bioactive molecules, both in terms of quantity and usefulness for food web and ecosystem productivity and functioning.

Data accessibility statement

All data have been made public and accessible in the Polar Data Catalogue; doi.org/10.21963/13258.

Supplemental files

The supplemental files for this article can be found as follows:

Figures S1 and S2. png

Table S1. docx

Acknowledgments

This project is part of the NSERC-Manitoba Hydro funded Collaborative Research and Development (CRD) program known as BaySys. Data collection for this research would not have been possible without the support and hospitality of the CCGS Amundsen crew during the 2017 and 2018 field season. D.G. Babb was supported through an NSERC PGS-D, the Canadian Meteorological and Oceanographic Society (CMOS) and D. Barber's Canada Research Chair funding. NSERC discovery grant funding (DI) supported research specific to this work, as did the University of Manitoba Graduate Fellowship (UMGF) and the Northern Scientific Training Program (NSTP). This work is a contribution to the ArcticNet Networks of Centres of Excellence and the Arctic Science Partnership (ASP, asp-net.org). We would like to thank the Sentinel North Research Project BriGHT, Amundsen Science and Québec-Océan for their contribution in sampling time, polar logistic and scientific equipment. We thank all of the participants in the BaySys campaign for their contribution to the fieldwork and data collection. This research was supported by the Sentinel North program of Université Laval, made possible, in part, thanks to funding from the Canada First Research Excellence Fund. We are grateful to the two anonymous reviewers for providing useful and constructive comments on a previous version of the manuscript.

Funding

This research was supported by the Sentinel North program of Université Laval, made possible, in part, thanks to funding from the Canada First Research Excellence Fund. Funding for this research was also graciously provided by Manitoba Hydro, the Natural Sciences and Engineering Research Council of Canada, Amundsen Science, and the Canada Research Chairs program.

Competing interests

The authors declare that they have no competing interests. Jean-Eric Tremblay is an associate editor at *Elementa*. He was not involved in the review process of this manuscript.

Author contributions

Contributed to conception and design: RA, JL, J-ET.

Contributed to acquisition of data: KC-B, LCM, IP, CJM, DGB.

Contributed to analysis and interpretation of data: RA, JL.

Drafted and/or revised the article: RA, JL, J-ET, KC-B, LCM, IP, CJM, DGB.

Approved the submitted version for publication: RA, JL, J-ET, KC-B, LCM, IP, CJM, DGB.

References

Alou-Font, E, **Roy, S**, **Agustí, S**, **Gosselin, M**. 2016. Cell viability, pigments and photosynthetic performance of Arctic phytoplankton in contrasting ice-covered and open-water conditions during the spring-summer transition. *Marine Ecology Progress Series* **543**: 89–106. DOI: http://dx.doi.org/10.3354/meps11562.

Amiraux, R, **Archambault, P**, **Moriceau, B**, **Lemire, M**, **Babin, M**, **Memery, L**, **Massé, G**, **Tremblay, J-E**. 2020. Efficiency of sympagic-benthic coupling revealed by analyses of n-3 fatty acids, IP25 and other highly branched isoprenoids in two filter-feeding Arctic benthic molluscs: *Mya truncata* and *Serripes groenlandicus*. *Organic Geochemistry* **151**: 104160. DOI: http://dx.doi.org/10.1016/j.orggeochem.2020.104160.

Andrews, J, **Babb, D**, **Barber, DG**, **Ackley, SF**. 2018. Climate change and sea ice: Shipping in Hudson Bay, Hudson Strait, and Foxe Basin (1980–2016). *Elementa: Science of the Anthropocene* **6**. DOI: http://dx.doi.org/10.1525/elementa.281.

Ardyna, M, **Babin, M**, **Devred, E**, **Forest, A**, **Gosselin, M**, **Raimbault, P**, **Tremblay, JÉ**. 2017. Shelf-basin gradients shape ecological phytoplankton niches and community composition in the coastal Arctic Ocean (Beaufort Sea). *Limnology and Oceanography* **62**(5): 2113–2132. DOI: http://dx.doi.org/10.1002/lno.10554.

Ardyna, M, **Mundy, C**, **Mills, MM**, **Oziel, L**, **Grondin, P-L**, **Lacour, L**, **Verin, G**, **Van Dijken, G**, **Ras, J**, **Alou-Font, E**. 2020. Environmental drivers of under-ice phytoplankton bloom dynamics in the Arctic Ocean. *Elementa: Science of the Anthropocene* **8**. DOI: http://dx.doi.org/10.1525/elementa.430.

Astorg, P, **Gradelet, S**, **Bergès, R**, **Suschetet, M**. 1997. Dietary lycopene decreases the initiation of liver preneoplastic foci by diethylnitrosamine in the rat. *Nutrition and Cancer* **29**(1): 60–68. DOI: http://dx.doi.org/10.1080/01635589709514603.

Bérard-Therriault, L, **Poulin, M**, **Bossé, L**. 1999. *Guide d'identification du phytoplancton marin de l'estuaire et du golfe du Saint-Laurent: Incluant également certains protozoaires*. Ottawa, Canada: NRC Research Press.

Blanchet, FG, **Legendre, P**, **Borcard, D**. 2008. Forward selection of explanatory variables. *Ecology* **89**(9): 2623–2632. DOI: http://dx.doi.org/10.1890/07-0986.1.

Brunet, C, **Johnsen, G**, **Lavaud, J**, **Roy, S**. 2011. Pigments and photoacclimation processes. *Phytoplankton Pigments: Characterization, Chemotaxonomy and Applications in Oceanography*. HAL Id: hal-01101814. Available at https://hal.archives-ouvertes.fr/hal-01101814. Accessed July 15, 2021.

Brunet, T, **Larson, BT**, **Linden, TA**, **Vermeij, MJ**, **McDonald, K**, **King, N**. 2019. Light-regulated collective contractility in a multicellular choanoflagellate. *Science* **366**(6463): 326–334. DOI: http://dx.doi.org/10.1126/science.aay2346.

Calder, PC. 2014. Very long chain omega-3 (n-3) fatty acids and human health. *European Journal of Lipid Science and Technology* **116**(10): 1280–1300. DOI: http://dx.doi.org/10.1002/ejlt.201400025.

Campanyà-Llovet, N, **Snelgrove, PV**, **Parrish, CC**. 2017. Rethinking the importance of food quality in marine benthic food webs. *Progress in Oceanography* **156**: 240–251. DOI: http://dx.doi.org/10.1016/j.pocean.2017.07.006.

Campbell, K, **Mundy, C**, **Landy, J**, **Delaforge, A**, **Michel, C**, **Rysgaard, S**. 2016. Community dynamics of bottom-ice algae in Dease Strait of the Canadian Arctic. *Progress in Oceanography* **149**: 27–39. DOI: http://dx.doi.org/10.1016/j.pocean.2016.10.005.

Chassot, E, **Bonhommeau, S**, **Dulvy, NK**, **Mélin, F**, **Watson, R**, **Gascuel, D**, **Le Pape, O**. 2010. Global marine primary production constrains fisheries catches. *Ecology Letters* **13**(4): 495–505. DOI: http://dx.doi.org/10.1111/j.1461-0248.2010.01443.x.

Coelho, LF, **Couceiro, JF**, **Keller-Costa, T**, **Valente, SM**, **Ramalho, TP**, **Carneiro, J**, **Comte, J**, **Blais, M-A**, **Vincent, WF**, **Martins, Z**. 2022. Structural shifts in sea ice prokaryotic communities across a salinity gradient in the subarctic. *Science of the Total Environment* **827**: 154286. DOI: http://dx.doi.org/10.1016/j.scitotenv.2022.154286.

Coupel, P, **Matsuoka, A**, **Ruiz-Pino, D**, **Gosselin, M**, **Marie, D**, **Tremblay, J-É**, **Babin, M**. 2015. Pigment signatures of phytoplankton communities in the Beaufort Sea. *Biogeosciences* **12**(4): 991–1006. DOI: http://dx.doi.org/10.5194/bg-12-991-2015.

Croteau, D, **Guérin, S**, **Bruyant, F**, **Ferland, J**, **Campbell, DA**, **Babin, M**, **Lavaud, J**. 2021. Contrasting non-photochemical quenching patterns under high light and darkness aligns with light niche occupancy in Arctic diatoms. *Limnology and Oceanography* **66**: S231–S245. DOI: http://dx.doi.org/10.1002/lno.11587.

D'Amico, S, **Collins, T**, **Marx, JC**, **Feller, G**, **Gerday, C**, **Gerday, C**. 2006. Psychrophilic microorganisms: Challenges for life. *EMBO Reports* **7**(4): 385–389. DOI: http://dx.doi.org/10.1038/sj.embor.7400662.

D'Orazio, N, **Gammone, MA**, **Gemello, E**, **De Girolamo, M**, **Cusenza, S**, **Riccioni, G**. 2012. Marine bioactives: Pharmacological properties and potential applications against inflammatory diseases. *Marine Drugs* **10**(4): 812–833. DOI: http://dx.doi.org/10.3390/md10040812.

Derksen, C, **Burgess, D**, **Duguay, C**, **Howell, S**, **Mudryk, L**, **Smith, S**, **Thackeray, C**, **Kirchmeier-Young, M**. 2019. Changes in snow, ice, and permafrost across Canada, in Bush, E, Lemmen, DS eds., *Canada's changing climate report*. Ottawa, Canada: Government of Canada: 194–260.

Déry, SJ, **Stadnyk, TA**, **MacDonald, MK**, **Gauli-Sharma, B**. 2016. Recent trends and variability in river discharge across northern Canada. *Hydrology and Earth System Sciences* **20**(12): 4801–4818. DOI: http://dx.doi.org/10.5194/hess-20-4801-2016.

Duncan, RJ, **Nielsen, DA**, **Sheehan, CE**, **Deppeler, S**, **Hancock, AM**, **Schulz, KG**, **Davidson, AT**, **Petrou, K**. 2022. Ocean acidification alters the nutritional value of Antarctic diatoms. *New Phytologist* **233**(4): 1813–1827. DOI: http://dx.doi.org/10.1111/nph.17868.

Dunstan, GA, **Volkman, JK**, **Barrett, SM**, **Leroi, JM**, **Jeffrey, SW**. 1994. Essential polyunsaturated fatty acids from 14 species of diatom (Bacillariophyceae). *Phytochemistry* **35**(1): 155–161. DOI: http://dx.doi.org/10.1016/S0031-9422(00)90525-9.

Dunstan, JA, **Mitoulas, LR**, **Dixon, G**, **Doherty, DA**, **Hartmann, PE**, **Simmer, K**, **Prescott, SL**. 2007. The effects of fish oil supplementation in pregnancy on breast milk fatty acid composition over the course of lactation: A randomized controlled trial. *Pediatric Research* **62**(6): 689–694. DOI: http://dx.doi.org/10.1203/PDR.0b013e318159a93a.

Egeland, ES. 2016. Carotenoids, in Borowitzka MA, Beardall J, Raven JA eds., *The physiology of microalgae*. Cham, Switzerland: Springer International Publishing: 507–563.

Erdinest, N, **Shmueli, O**, **Grossman, Y**, **Ovadia, H**, **Solomon, A**. 2012. Anti-inflammatory effects of alpha linolenic acid on human corneal epithelial cells. *Investigative Ophthalmology & Visual Science* **53**(8): 4396–4406. DOI: http://dx.doi.org/10.1167/iovs.12-9724.

Fan, Y-Y, **Chapkin, RS**. 1998. Importance of dietary γ-linolenic acid in human health and nutrition. *The Journal of Nutrition* **128**(9): 1411–1414. DOI: http://dx.doi.org/10.1093/jn/128.9.1411.

Fuschino, JR, **Guschina, IA**, **Dobson, G**, **Yan, ND**, **Harwood, JL**, **Arts, MT**. 2011. Rising water temperatures alter lipid dynamics and reduce n-3 essential fatty acid concentrations in *Scenedesmus obliquus* (chlorophyta). *Journal of Phycology* **47**(4): 763–774. DOI: http://dx.doi.org/10.1111/j.1529-8817.2011.01024.x.

Gagnon, AS, **Gough, WA**. 2005. Trends in the dates of ice freeze-up and breakup over Hudson Bay, Canada. *Arctic* **58**(4): 370–382.

Galasso, C, **Corinaldesi, C**, **Sansone, C**. 2017. Carotenoids from marine organisms: Biological functions and industrial applications. *Antioxidants* **6**(4): 96. DOI: http://dx.doi.org/10.3390/antiox6040096.

Galasso, C, **Gentile, A**, **Orefice, I**, **Ianora, A**, **Bruno, A**, **Noonan, DM**, **Sansone, C**, **Albini, A**, **Brunet, C**. 2019. Microalgal derivatives as potential nutraceutical and food supplements for human health: A focus on cancer prevention and interception. *Nutrients* **11**(6): 1226. DOI: http://dx.doi.org/10.3390/nu11061226.

Galindo, V, **Gosselin, M**, **Lavaud, J**, **Mundy, CJ**, **Else, B**, **Ehn, J**, **Babin, M**, **Rysgaard, S**. 2017. Pigment composition and photoprotection of Arctic sea ice algae during spring. *Marine Ecology Progress Series* **585**: 49–69. DOI: http://dx.doi.org/10.3354/meps12398.

Guschina, IA, **Harwood, JL**. 2006. Lipids and lipid metabolism in eukaryotic algae. *Progress in Lipid Research* **45**(2): 160–186. DOI: http://dx.doi.org/10.1016/j.plipres.2006.01.001.

Hansen, H, **Koroleff, F**, **Grasshoff, K**, **Kremling, K**, **Ehrhardt, M**. 1999. *Methods of seawater analysis*. New York, NY: John Wiley & Sons.

Hendriks, IE, **van Duren, LA**, **Herman, PM**. 2003. Effect of dietary polyunsaturated fatty acids on reproductive output and larval growth of bivalves. *Journal of Experimental Marine Biology and Ecology* **296**(2): 199–213. DOI: http://dx.doi.org/10.1016/S0022-0981(03)00323-X.

Hixson, SM, **Arts, MT**. 2016. Climate warming is predicted to reduce omega-3, long-chain, polyunsaturated fatty acid production in phytoplankton. *Global Change Biology* **22**(8): 2744–2755. DOI: http://dx.doi.org/10.1111/gcb.13295.

Hochheim, K, **Barber, D**. 2010. Atmospheric forcing of sea ice in Hudson Bay during the fall period, 1980–2005. *Journal of Geophysical Research: Oceans* **115**(C5). DOI: http://dx.doi.org/10.1029/2009JC005334.

Hochheim, KP, **Barber, DG**. 2014. An update on the ice climatology of the Hudson Bay system. *Arctic, Antarctic, and Alpine Research* **46**(1): 66–83. DOI: http://dx.doi.org/10.1657/1938-4246-46.1.66.

Hoover, C, **Pitcher, T**, **Christensen, V**. 2013. Effects of hunting, fishing and climate change on the Hudson Bay marine ecosystem: II. Ecosystem model future projections. *Ecological Modelling* **264**: 143–156. DOI: http://dx.doi.org/10.1016/j.ecolmodel.2013.01.010.

Huang, JJ, **Lin, S**, **Xu, W**, **Cheung, PCK**. 2017. Occurrence and biosynthesis of carotenoids in phytoplankton. *Biotechnology Advances* **35**(5): 597–618. DOI: http://dx.doi.org/10.1016/j.biotechadv.2017.05.001.

Ingram, R, **Prinsenberg, S**. 1998. Coastal oceanography of Hudson Bay and surrounding eastern Canadian Arctic waters. *The Sea* **11**(29): 835–859.

Intergovernmental Panel on Climate Change. 2014. Climate change 2014: Impacts, adaptation, and vulnerability. Part B: Regional aspects, in Barros, VR, Field, CB, Dokken, DJ, Mastrandrea, MD, Mach, KJ, Bilir, TE, Chatterjee, M, Ebi, KL, Estrada, YO, Genova, RC, Girma, B, Kissel, ES, Levy, AN, MacCracken, S, Mastrandrea, PR, White, LL eds., *Contribution of Working Group II to the Fifth Assessment Report of the Intergovernmental Panel on Climate Change*. Cambridge, UK: Cambridge University Press: 1371–1438.

Jin, P, **Hutchins, DA**, **Gao, K**. 2020. The impacts of ocean acidification on marine food quality and its potential food chain consequences. *Frontiers in Marine Science* **7**: 543979. DOI: http://dx.doi.org/10.3389/fmars.2020.543979.

Johansen, J, **Svec, W**, **Liaaen-Jensen, S**, **Haxo, F**. 1974. Carotenoids of the dinophyceae. *Phytochemistry* **13**(10): 2261–2271. DOI: http://dx.doi.org/10.1016/0031-9422(74)85038-7.

Katiyar, R, **Arora, A**. 2020. Health promoting functional lipids from microalgae pool: A review. *Algal*

Research **46**: 101800. DOI: http://dx.doi.org/10.1016/j.algal.2020.101800.

Kauko, HM, **Pavlov, AK**, **Johnsen, G**, **Granskog, MA**, **Peeken, I**, **Assmy, P**. 2019. Photoacclimation state of an Arctic underice phytoplankton bloom. *Journal of Geophysical Research: Oceans* **124**(3): 1750–1762. DOI: http://dx.doi.org/10.1029/2018JC014777.

Kelly, JR, **Scheibling, RE**. 2012. Fatty acids as dietary tracers in benthic food webs. *Marine Ecology Progress Series* **446**: 1–22. DOI: http://dx.doi.org/10.3354/meps09559.

Kirillov, S, **Babb, D**, **Dmitrenko, I**, **Landy, J**, **Lukovich, J**, **Ehn, J**, **Sydor, K**, **Barber, D**, **Stroeve, J**. 2020. Atmospheric forcing drives the winter sea ice thickness asymmetry of Hudson Bay. *Journal of Geophysical Research: Oceans* **125**(2): e2019JC015756. DOI: http://dx.doi.org/10.1029/2019JC015756.

Krause, JW, **Duarte, CM**, **Marquez, IA**, **Assmy, P**, **Fernández-Méndez, M**, **Wiedmann, I**, **Wassmann, P**, **Kristiansen, S**, **Agustí, S**. 2018. Biogenic silica production and diatom dynamics in the Svalbard region during spring. *Biogeosciences* **15**(21): 6503–6517. DOI: http://dx.doi.org/10.5194/bg-15-6503-2018.

Krause, JW, **Schulz, IK**, **Rowe, KA**, **Dobbins, W**, **Winding, MH**, **Sejr, MK**, **Duarte, CM**, **Agustí, S**. 2019. Silicic acid limitation drives bloom termination and potential carbon sequestration in an Arctic bloom. *Scientific Reports* **9**(1): 1–11. DOI: http://dx.doi.org/10.1038/s41598-019-44587-4.

Kuczynska, P, **Jemiola-Rzeminska, M**, **Strzalka, K**. 2015. Photosynthetic pigments in diatoms. *Marine Drugs* **13**(9): 5847–5881. DOI: http://dx.doi.org/10.3390/md13095847.

Kuzyk, Z, **Candlish, L**. 2019. *From science to policy in the Greater Hudson Bay Marine Region: An Integrated Regional Impact Study (IRIS) of climate change and modernization*. Québec, Canada: University Laval.

Lacour, T, **Babin, M**, **Lavaud, J**. 2020. Diversity in xanthophyll cycle pigments content and related nonphotochemical quenching (NPQ) among microalgae: Implications for growth strategy and ecology. *Journal of Phycology* **56**(2): 245–263. DOI: http://dx.doi.org/10.1111/jpy.12944.

Lalande, C, **Bauerfeind, E**, **Nöthig, E-M**, **Beszczynska-Möller, A**. 2013. Impact of a warm anomaly on export fluxes of biogenic matter in the eastern Fram Strait. *Progress in Oceanography* **109**: 70–77. DOI: http://dx.doi.org/10.1016/j.pocean.2012.09.006.

Landy, JC, **Ehn, JK**, **Babb, DG**, **Thériault, N**, **Barber, DG**. 2017. Sea ice thickness in the Eastern Canadian Arctic: Hudson Bay Complex & Baffin Bay. *Remote Sensing of Environment* **200**: 281–294. DOI: http://dx.doi.org/10.1016/j.rse.2017.08.019.

Lee, SH, **Whitledge, TE**. 2005. Primary and new production in the deep Canada Basin during summer 2002. *Polar Biology* **28**(3): 190–197. DOI: http://dx.doi.org/10.1007/s00300-004-0676-3.

Leonardos, N, **Lucas, IA**. 2000. The nutritional value of algae grown under different culture conditions for *Mytilus edulis* L. larvae. *Aquaculture* **182**(3–4): 301–315. DOI: http://dx.doi.org/10.1016/S0044-8486(99)00269-0.

Leu, E, **Falk-Petersen, S**, **Kwaśniewski, S**, **Wulff, A**, **Edvardsen, K**, **Hessen, DO**. 2006. Fatty acid dynamics during the spring bloom in a High Arctic fjord: Importance of abiotic factors versus community changes. *Canadian Journal of Fisheries and Aquatic Sciences* **63**(12): 2760–2779. DOI: http://dx.doi.org/10.1139/f06-159.

Leu, E, **Graeve, M**, **Wulff, A**. 2016. A (too) bright future? Arctic diatoms under radiation stress. *Polar Biology* **39**(10): 1711–1724. DOI: http://dx.doi.org/10.1007/s00300-016-2003-1.

Leu, E, **Søreide, JE**, **Hessen, DO**, **Falk-Petersen, S**, **Berge, J**. 2011. Consequences of changing sea-ice cover for primary and secondary producers in the European Arctic shelf seas: Timing, quantity, and quality. *Progress in Oceanography* **90**(1–4): 18–32. DOI: http://dx.doi.org/10.1016/j.pocean.2011.02.004.

Leu, E, **Wiktor, J**, **søreide, JE**, **Berge, J**, **Falk-Petersen, S**. 2010. Increased irradiance reduces food quality of sea ice algae. *Marine Ecology Progress Series* **411**: 49–60. DOI: http://dx.doi.org/10.3354/meps08647.

Lewis, K, **Van Dijken, G**, **Arrigo, K**. 2020. Changes in phytoplankton concentration now drive increased Arctic Ocean primary production. *Science* **369**(6500): 198–202. DOI: http://dx.doi.org/10.1126/science.aay8380.

Li, WK, **McLaughlin, FA**, **Lovejoy, C**, **Carmack, EC**. 2009. Smallest algae thrive as the Arctic Ocean freshens. *Science* **326**(5952): 539–539. DOI: http://dx.doi.org/10.1126/science.1179798.

Lund, J, **Kipling, C**, **Le Cren, E**. 1958. The inverted microscope method of estimating algal numbers and the statistical basis of estimations by counting. *Hydrobiologia* **11**(2): 143–170. DOI: http://dx.doi.org/10.1007/BF00007865.

Marmillot, V, **Parrish, CC**, **Tremblay, J-É**, **Gosselin, M**, **MacKinnon, JF**. 2020. Environmental and biological determinants of algal lipids in western Arctic and subarctic seas. *Frontiers in Environmental Science* **8**: 538635. DOI: http://dx.doi.org/10.3389/fenvs.2021.655241.

Matthes, L, **Ehn, J**, **Dalman, L**, **Babb, D**, **Peeken, I**, **Harasyn, M**, **Kirillov, S**, **Lee, J**, **Bélanger, S**, **Tremblay, J-É**. 2021. Environmental drivers of spring primary production in Hudson Bay. *Elementa: Science of the Anthropocene* **9**(1): 00160. DOI: http://dx.doi.org/10.1525/elementa.2020.00160.

McKenzie, C, **Deibel, D**, **Thompson, R**, **MacDonald, B**, **Penney, R**. 1997. Distribution and abundance of choanoflagellates (Acanthoecidae) in the coastal cold ocean of Newfoundland, Canada. *Marine Biology* **129**(3): 407–416. DOI: http://dx.doi.org/10.1007/s002270050181.

Micallef, MA, **Garg, ML**. 2009. Beyond blood lipids: Phytosterols, statins and omega-3 polyunsaturated fatty acid therapy for hyperlipidemia. *The Journal of Nutritional Biochemistry* **20**(12): 927–939. DOI: http://dx.doi.org/10.1016/j.jnutbio.2009.06.009.

Napolitano, GE, **Ackman, RG**, **Ratnayake, WM**. 1990. Fatty acid composition of three cultured algal species (*Isochvysis galbana*, *Chaetoceros gracilis* and *Chaetoceros calcitrans*) used as food for bivalve larvae. *Journal of the World Aquaculture Society* **21**(2): 122–130. DOI: http://dx.doi.org/10.1111/j.1749-7345.1990.tb00532.x.

Nichols, DS. 2003. Prokaryotes and the input of polyunsaturated fatty acids to the marine food web. *FEMS Microbiology Letters* **219**(1): 1–7. DOI: http://dx.doi.org/10.1016/S0378-1097(02)01200-4.

Nicolaus, M, **Katlein, C**, **Maslanik, J**, **Hendricks, S**. 2012. Changes in Arctic sea ice result in increasing light transmittance and absorption. *Geophysical Research Letters* **39**(24). DOI: http://dx.doi.org/10.1029/2012GL053738.

Nöthig, E-M, **Bracher, A**, **Engel, A**, **Metfies, K**, **Niehoff, B**, **Peeken, I**, **Bauerfeind, E**, **Cherkasheva, A**, **Gäbler-Schwarz, S**, **Hardge, K**, **Kilias, E**, **Kraft, A**, **Mebrahtom Kidane, Y**, **Lalande, C**, **Piontek, J**, **Thomisch, K**, **Wurst, M**. 2015. Summertime plankton ecology in Fram Strait—A compilation of long- and short-term observations. *Polar Research* **34**(1): 23349. DOI: http://dx.doi.org/10.3402/polar.v34.23349.

Oksanen, J, **Blanchet, F**, **Kindt, R**, **Legendre, P**, **Minchin, P**, **O'Hara, R**, **Simpson, G**, **Solymos, P**, **Stevens, M**, **Wagner, H**. 2015. *Vegan: Community ecology package. R package vegan, Version 2.2-1*. Nairobi, Kenya: World Agroforestry Centre.

Paiva, SA, **Russell, RM**. 1999. β-carotene and other carotenoids as antioxidants. *Journal of the American College of Nutrition* **18**(5): 426–433. DOI: http://dx.doi.org/10.1080/07315724.1999.10718880.

Parkinson, C, **Gloersen, P**, **Zwally, H**, **Cavalieri, D**, **Meier, W**, **Fetterer, F**, **Knowles, K**, **Savoie, M**, **Brodzik, M**. 1996, Updated yearly. *Sea ice concentrations from Nimbus-7 SMMR and DMSP SSM/I-SSMIS Passive Microwave Data, Version 1*. Boulder, CO: NASA National Snow and Ice Data Center Distributed Active Archive Center. DOI: http://dx.doi.org/10.5067/8GQ8LZQVL0VL.

Parsons, T, **Maita, Y**, **Lalli, C**. 1984. *A manual of chemical and biological methods for seawater analysis*. Toronto, Canada: Pergamon Press.

Paulic, J, **Rice, J**. 2011. Identification of ecologically and biologically significant areas (EBSAs) in the Canadian Arctic. *Proceedings Series*: 047. Available at https://publications.gc.ca/collections/collection_2012/mpo-dfo/Fs70-4-2011-047.pdf. Accessed July 20, 2021.

Peng, J, **Yuan, J-P**, **Wu, C-F**, **Wang, J-H**. 2011. Fucoxanthin, a marine carotenoid present in brown seaweeds and diatoms: Metabolism and bioactivities relevant to human health. *Marine Drugs* **9**(10): 1806–1828. DOI: http://dx.doi.org/10.3390/md9101806.

Piepho, M, **Arts, MT**, **Wacker, A**. 2012. Species-specific variation in fatty acid concentrations of four phytoplankton species: Does phosphorus supply influence the effect of light intensity or temperature? *Journal of Phycology* **48**(1): 64–73. DOI: http://dx.doi.org/10.1111/j.1529-8817.2011.01103.x.

Popova, E, **Yool, A**, **Coward, A**, **Aksenov, Y**, **Alderson, S**, **De Cuevas, B**, **Anderson, T**. 2010. Control of primary production in the Arctic by nutrients and light: Insights from a high resolution ocean general circulation model. *Biogeosciences* **7**(11): 3569–3591. DOI: http://dx.doi.org/10.5194/bgd-7-5557-2010.

Poulin, M, **Daugbjerg, N**, **Gradinger, R**, **Ilyash, L**, **Ratkova, T**, **Von Quillfeldt, C**. 2011. The pan-Arctic biodiversity of marine pelagic and sea-ice unicellular eukaryotes: A first-attempt assessment. *Marine Biodiversity* **41**(1): 13–28. DOI: http://dx.doi.org/10.1007/s12526-010-0058-8.

Prinsenberg, S. 1986. The circulation pattern and current structure of Hudson Bay. *Elsevier Oceanography Series* **44**: 187–204. DOI: http://dx.doi.org/10.1016/S0422-9894(08)70903-6.

Quinn, GP, **Keough, M**. 2002. *Experimental design and data analysis for biologists*. Cambridge, UK: Cambridge University Press.

R Core Team. 2018. R: A language and environment for statistical computing. Vienna, Austria: R Foundation for Statistical Computing. Available at https://www.R-project.org.

Rao, AV, **Rao, LG**. 2007. Carotenoids and human health. *Pharmacological Research* **55**(3): 207–216. DOI: http://dx.doi.org/10.1016/j.phrs.2007.01.012.

Rao, CR. 1964. The use and interpretation of principal component analysis in applied research. *Sankhyā: The Indian Journal of Statistics, Series A*: 329–358.

Ras, J, **Claustre, H**, **Uitz, J**. 2008. Spatial variability of phytoplankton pigment distributions in the Subtropical South Pacific Ocean: Comparison between in situ and predicted data. *Biogeosciences* **5**(2): 353–369. DOI: http://dx.doi.org/10.5194/bg-5-353-2008.

Ridenour, NA, **Hu, X**, **Sydor, K**, **Myers, PG**, **Barber, DG**. 2019. Revisiting the circulation of Hudson Bay: Evidence for a seasonal pattern. *Geophysical Research Letters* **46**(7): 3891–3899. DOI: http://dx.doi.org/10.1029/2019GL082344.

Robertson, R, **Guihéneuf, F**, **Schmid, M**, **Stengel, DB**, **Fitzgerald, G**, **Ross, P**, **Stanton, C**. 2013. *Algae-derived polyunsaturated fatty acids: Implications for human health*. Hauppauge, NY: Nova Sciences Publishers, Inc.

Rousch, JM, **Bingham, SE**, **Sommerfeld, MR**. 2003. Changes in fatty acid profiles of thermo-intolerant and thermo-tolerant marine diatoms during temperature stress. *Journal of Experimental Marine Biology and Ecology* **295**(2): 145–156. DOI: http://dx.doi.org/10.1016/S0022-0981(03)00293-4.

Ruiz-López, N, **Haslam, RP**, **Venegas-Calerón, M**, **Li, T**, **Bauer, J**, **Napier, JA**, **Sayanova, O**. 2012. Enhancing the accumulation of omega-3 long chain polyunsaturated fatty acids in transgenic *Arabidopsis thaliana* via iterative metabolic engineering and genetic crossing. *Transgenic Research* **21**(6):

1233–1243. DOI: http://dx.doi.org/10.1007/s11248-012-9596-0.

Sansone, C, **Brunet, C**. 2020. Marine algal antioxidants. *Antioxidants* **9**(3): 206.

Saucier, F, **Senneville, S**, **Prinsenberg, S**, **Roy, F**, **Smith, G**, **Gachon, P**, **Caya, D**, **Laprise, R**. 2004. Modelling the sea ice-ocean seasonal cycle in Hudson Bay, Foxe Basin and Hudson Strait, Canada. *Climate Dynamics* **23**(3-4): 303–326. DOI: http://dx.doi.org/10.1007/s00382-004-0445-6.

Schmidt, EB, **Dyerberg, J**. 1994. Omega-3 fatty acids. *Drugs* **47**(3): 405–424. DOI: http://dx.doi.org/10.2165/00003495-199447030-00003.

Shahidi, F, **Ambigaipalan, P**. 2018. Omega-3 polyunsaturated fatty acids and their health benefits. *Annual Review of Food Science and Technology* **9**: 345–381. DOI: http://dx.doi.org/10.1146/annurev-food-111317-095850.

Shivaji, S, **Prakash, JS**. 2010. How do bacteria sense and respond to low temperature? *Archives of Microbiology* **192**(2): 85–95. DOI: http://dx.doi.org/10.1007/s00203-009-0539-y.

Sinensky, M. 1974. Homeoviscous adaptation—A homeostatic process that regulates the viscosity of membrane lipids in *Escherichia coli*. *Proceedings of the National Academy of Sciences* **71**(2): 522–525. DOI: http://dx.doi.org/10.1073/pnas.71.2.522.

Smith, GI, **Atherton, P**, **Reeds, DN**, **Mohammed, BS**, **Rankin, D**, **Rennie, MJ**, **Mittendorfer, B**. 2011. Dietary omega-3 fatty acid supplementation increases the rate of muscle protein synthesis in older adults: A randomized controlled trial. *The American Journal of Clinical Nutrition* **93**(2): 402–412. DOI: http://dx.doi.org/10.3945/ajcn.110.005611.

Solovchenko, A, **Merzlyak, M**. 2008. Screening of visible and UV radiation as a photoprotective mechanism in plants. *Russian Journal of Plant Physiology* **55**(6): 719–737. DOI: http://dx.doi.org/10.1134/S1021443708060010.

Søreide, JE, **Falk-Petersen, S**, **Hegseth, EN**, **Hop, H**, **Carroll, ML**, **Hobson, KA**, **Blachowiak-Samolyk, K**. 2008. Seasonal feeding strategies of *Calanus* in the high-Arctic Svalbard region. *Deep Sea Research Part II Topical Studies in Oceanography* **55**(20–21): 2225–2244. DOI: http://dx.doi.org/10.1016/j.dsr2.2008.05.024.

Søreide, JE, **Leu, E**, **Berge, J**, **Graeve, M**, **Falk-Petersen, S**. 2010. Timing of blooms, algal food quality and *Calanus glacialis* reproduction and growth in a changing Arctic. *Global Change Biology* **16**(11): 3154–3163. DOI: http://dx.doi.org/10.1111/j.1365-2486.2010.02175.x.

Stewart, D, **Barber, D**. 2010. The ocean-sea ice-atmosphere system of the Hudson Bay complex, in Ferguson, SH, Loseto, LL, Mallory, ML eds., *A little less Arctic.* Dordrecht, the Netherlands: Springer: 1–38. Available at https://doi.org/10.1007/978-90-481-9121-5_1.

Strom, SL, **Fredrickson, KA**. 2008. Intense stratification leads to phytoplankton nutrient limitation and reduced microzooplankton grazing in the southeastern Bering Sea. *Deep Sea Research Part II: Topical Studies in Oceanography* **55**(16–17): 1761–1774. DOI: http://dx.doi.org/10.1016/j.dsr2.2008.04.008.

Šupraha, L, **Bosak, S**, **Ljubešić, Z**, **Mihanović, H**, **Olujić, G**, **Mikac, I**, **Viličić, D**. 2014. Cryptophyte bloom in a Mediterranean estuary: High abundance of *Plagioselmis* cf. *prolonga* in the Krka River estuary (eastern Adriatic Sea). *Scientia Marina* **78**: 329–338.

Terhaar, J, **Lauerwald, R**, **Regnier, P**, **Gruber, N**, **Bopp, L**. 2021. Around one third of current Arctic Ocean primary production sustained by rivers and coastal erosion. *Nature Communications* **12**(1): 1–10. DOI: http://dx.doi.org/10.1038/s41467-020-20470-z.

Thaler, M, **Lovejoy, C**. 2015. Biogeography of heterotrophic flagellate populations indicates the presence of generalist and specialist taxa in the Arctic Ocean. *Applied and Environmental Microbiology* **81**(6): 2137–2148. DOI: http://dx.doi.org/10.1128/AEM.02737-14.

Thomson, PG, **Wright, SW**, **Bolch, CJ**, **Nichols, PD**, **Skerratt, JH**, **McMinn, A**. 2004. Antarctic distribution, pigment and lipid composition, and molecular identification of the brine dinoflagellate *Polarella glacialis* (dinophyceae). *Journal of Phycology* **40**(5): 867–873. DOI: http://dx.doi.org/10.1111/j.1529-8817.2004.03169.x.

Throndsen, J, **Hasle, GR**, **Tangen, K**. 2007. *Phytoplankton of Norwegian coastal waters*. Oslo, Norway: Almater Forlag AS.

Tivy, A, **Howell, SE**, **Alt, B**, **Yackel, JJ**, **Carrieres, T**. 2011. Origins and levels of seasonal forecast skill for sea ice in Hudson Bay using canonical correlation analysis. *Journal of Climate* **24**(5): 1378–1395. DOI: http://dx.doi.org/10.1175/2010JCLI3527.1.

Tomas, CR. 1997. *Identifying marine phytoplankton*. San Diego, CA: Academic Press.

Tremblay, J-É, **Anderson, LG**, **Matrai, P**, **Coupel, P**, **Bélanger, S**, **Michel, C**, **Reigstad, M**. 2015. Global and regional drivers of nutrient supply, primary production and CO_2 drawdown in the changing Arctic Ocean. *Progress in Oceanography* **139**: 171–196. DOI: http://dx.doi.org/10.1016/j.pocean.2015.08.009.

Tremblay, J-E, **Lee, J**, **Gosselin, M**, **Belanger, S**. 2019. Nutrient dynamic and marine biological productivity in the Greater Hudson Bay marine region, in Kuzyk, ZA, Candlish, LM eds., *From science to policy in the Greater Hudson Bay marine region: An integrated regional impact study (IRIS) of climate change and modernization*. Québec City, Canada: ArcticNet: 225–244.

Vallina, SM, **Follows, M**, **Dutkiewicz, S**, **Montoya, JM**, **Cermeno, P**, **Loreau, M**. 2014. Global relationship between phytoplankton diversity and productivity in the ocean. *Nature Communications* **5**(1): 1–10. DOI: http://dx.doi.org/10.1038/ncomms5299.

Vaquer-Sunyer, R, **Duarte, CM**, **Holding, J**, **Regaudie-de-Gioux, A**, **García-Corral, LS**, **Reigstad, M**, **Wassmann, P**. 2013. Seasonal patterns in Arctic planktonic metabolism (Fram Strait–Svalbard

region). *Biogeosciences* **10**(3): 1451–1469. DOI: http://dx.doi.org/10.5194/bg-10-1451-2013.

Viso, A-C, **Marty, J-C**. 1993. Fatty acids from 28 marine microalgae. *Phytochemistry* **34**(6): 1521–1533. DOI: http://dx.doi.org/10.1016/S0031-9422(00)90839-2.

Volkman, JK, **Jeffrey, SW**, **Nichols, PD**, **Rogers, GI**, **Garland, CD**. 1989. Fatty acid and lipid composition of 10 species of microalgae used in mariculture. *Journal of Experimental Marine Biology and Ecology* **128**(3): 219–240. DOI: http://dx.doi.org/10.1016/0022-0981(89)90029-4.

Wassmann, P, **Duarte, CM**, **Agusti, S**, **Sejr, MK**. 2011. Footprints of climate change in the Arctic marine ecosystem. *Global Change Biology* **17**(2): 1235–1249. DOI: http://dx.doi.org/10.1111/j.1365-2486.2010.02311.x.

Wassmann, P, **Ratkova, T**, **Andreassen, I**, **Vernet, M**, **Pedersen, G**, **Rey, F**. 1999. Spring bloom development in the marginal ice zone and the central Barents Sea. *Marine Ecology* **20**: 321–346. DOI: http://dx.doi.org/10.1046/j.1439-0485.1999.2034081.x.

Winter, R, **Dzwolak, W**. 2005. Exploring the temperature–pressure configurational landscape of biomolecules: From lipid membranes to proteins. *Philosophical Transactions of the Royal Society A: Mathematical, Physical and Engineering Sciences* **363**(1827): 537–563. DOI: http://dx.doi.org/10.1098/rsta.2004.1507.

Witman, JD, **Cusson, M**, **Archambault, P**, **Pershing, AJ**, **Mieszkowska, N**. 2008. The relation between productivity and species diversity in temperate–arctic marine ecosystems. *Ecology* **89**(sp11): S66–S80. DOI: http://dx.doi.org/10.1890/07-1201.1.

Xia, S, **Wang, K**, **Wan, L**, **Li, A**, **Hu, Q**, **Zhang, C**. 2013. Production, characterization, and antioxidant activity of fucoxanthin from the marine diatom *Odontella aurita*. *Marine Drugs* **11**(7): 2667–2681. DOI: http://dx.doi.org/10.3390/md11072667.

Yeum, K-J, **Aldini, G**, **Russell, RM**, **Krinsky, NI**. 2009. *Antioxidant/pro-oxidant actions of carotenoids*. Basel, Switzerland: Birkhäuser: 235–268. (Carotenoids series; vol. 5).

Yoon, HS, **Hackett, JD**, **Bhattacharya, D**. 2002. A single origin of the peridinin-and fucoxanthin-containing plastids in dinoflagellates through tertiary endosymbiosis. *Proceedings of the National Academy of Sciences* **99**(18): 11724–11729. DOI: http://dx.doi.org/10.1073/pnas.172234799.

How to cite this article: Amiraux, R, Lavaud, J, Cameron-Bergeron, K, Matthes, LC, Peeken, I, Mundy, CJ, Babb, DG, Tremblay, J-E. 2022. Content in fatty acids and carotenoids in phytoplankton blooms during the seasonal sea ice retreat in Hudson Bay complex, Canada. *Elementa: Science of the Anthropocene* 10(1). DOI: https://doi.org/10.1525/elementa.2021.00106

Domain Editor-in-Chief: Jody W. Deming, University of Washington, Seattle, WA, USA

Associate Editor: Kevin R. Arrigo, Department of Earth System Science, Stanford University, Stanford, CA, USA

Knowledge Domain: Ocean Science

Published: August 5, 2022 **Accepted:** July 13, 2022 **Submitted:** November 9, 2021